resources

MDPI

Article

Sources of Extraterrestrial Rare Earth Elements: To the Moon and Beyond

Claire L. McLeod [1,*] and Mark. P. S. Krekeler [2]

[1] Department of Geology and Environmental Earth Sciences, 203 Shideler Hall, Miami University, Oxford, OH 45056, USA

[2] Department of Geology and Environmental Earth Science, Miami University-Hamilton, Hamilton, OH 45011, USA; krekelmp@miamioh.edu

* Correspondence: mcleodcl@miamioh.edu; Tel.: 513-529-9662; Fax: 513-529-1542

Received: 10 June 2017; Accepted: 18 August 2017; Published: 23 August 2017

Abstract: The resource budget of Earth is limited. Rare-earth elements (REEs) are used across the world by society on a daily basis yet several of these elements have <2500 years of reserves left, based on current demand, mining operations, and technologies. With an increasing population, exploration of potential extraterrestrial REE resources is inevitable, with the Earth's Moon being a logical first target. Following lunar differentiation at ~4.50–4.45 Ga, a late-stage (after ~99% solidification) residual liquid enriched in Potassium (K), Rare-earth elements (REE), and Phosphorus (P), (or "KREEP") formed. Today, the KREEP-rich region underlies the Oceanus Procellarum and Imbrium Basin region on the lunar near-side (the Procellarum KREEP Terrain, PKT) and has been tentatively estimated at preserving 2.2×10^8 km^3 of KREEP-rich lithologies. The majority of lunar samples (Apollo, Luna, or meteoritic samples) contain REE-bearing minerals as trace phases, e.g., apatite and/or merrillite, with merrillite potentially contributing up to 3% of the PKT. Other lunar REE-bearing lunar phases include monazite, yittrobetafite (up to 94,500 ppm yttrium), and tranquillityite (up to 4.6 wt % yttrium, up to 0.25 wt % neodymium), however, lunar sample REE abundances are low compared to terrestrial ores. At present, there is no geological, mineralogical, or chemical evidence to support REEs being present on the Moon in concentrations that would permit their classification as ores. However, the PKT region has not yet been mapped at high resolution, and certainly has the potential to yield higher REE concentrations at local scales (<10s of kms). Future lunar exploration and mapping efforts may therefore reveal new REE deposits. Beyond the Moon, Mars and other extraterrestrial materials are host to REEs in apatite, chevkinite-perrierite, merrillite, whitlockite, and xenotime. These phases are relatively minor components of the meteorites studied to date, constituting <0.6% of the total sample. Nonetheless, they dominate a samples REE budget with their abundances typically 1–2 orders of magnitude enriched relative to their host rock. As with the Moon, though phases which host REEs have been identified, no extraterrestrial REE resource, or ore, has been identified yet. At present extraterrestrial materials are therefore not suitable REE-mining targets. However, they are host to other resources that will likely be fundamental to the future of space exploration and support the development of in situ resource utilization, for example: metals (Fe, Al, Mg, PGEs) and water.

Keywords: rare-earth elements; Moon; extraterrestrial; space; Mars; meteorites

1. Introduction

"Space may be vast, but many of the most valuable resources—especially those convenient to Earth—are limited. Our Moon may be one of the most promising sites for mining, energy capture, and spaceship refueling, but a limited amount of useable land exists, with an even more limited quantity of useable water. The problem is not limited to the Moon. Every resource is limited. The question then

is who, if anyone, should have the right to the riches of space? Space is an international zone, and so is, in a sense, the heritage of all humanity." [1]

The rare-earth elements (REEs) are a group of transition metals which include the lanthanide series of the periodic table (lanthanum to lutetium), in addition to scandium and yttrium. Despite the nomenclature, they are not rare with cerium (Ce) being the 25th most abundant element on Earth [2] at an average value of 60 ppm. This is compared to <1 ppm for the least abundant REEs (thulium (Tm) and lutetium (Lu)) [3]. In addition, the occurrence of REEs is often associated with U-Th mineralization, where uranium ore deposits often contain a significant concentration of REEs [4]. The REEs are as abundant as tin, lead, and cobalt in Earth's lithosphere, and are more abundant that gold and silver [5]. However, they are dispersed throughout the rock record and only exist in concentrated, economically viable, deposits in certain areas of the world with the largest accumulation of REEs being found in the Bayan Obo deposit in China [6].

The REEs are widely used on Earth by humankind on a daily basis. They are integral components of smart phones, computer monitors, flash drives, lightbulbs, camera lenses, catalysts, and magnets, and are fundamental to many military-based technologies. However, as of 2012, REEs had been produced from less than 20 minerals with bastnäsite ($REECO_3(F,OH)$), monazite ($(REE,Th,Ca,Sr)(P,Si,S)O_4$), xenotime ($(REE,Zr)(P,Si)O_4$), loparite ($(Na,REE,Ca)(Ti,Nb)O_3$), parisite ($CaREE_2(CO_3)_3(F,OH)_2$), and Al-clays, accounting for the majority of REE production [2]. From the USGS Mineral Commodity Summary in 2014 [7], Earth's REE reserves totaled 140 million tonnes, with almost half of those resources in China (55 million tonnes) and the United States (13 million tonnes). Figure 1 summarizes the years of REE reserves left on Earth based on recent mining practices and technologies, alongside their concentration in Earth's crust.

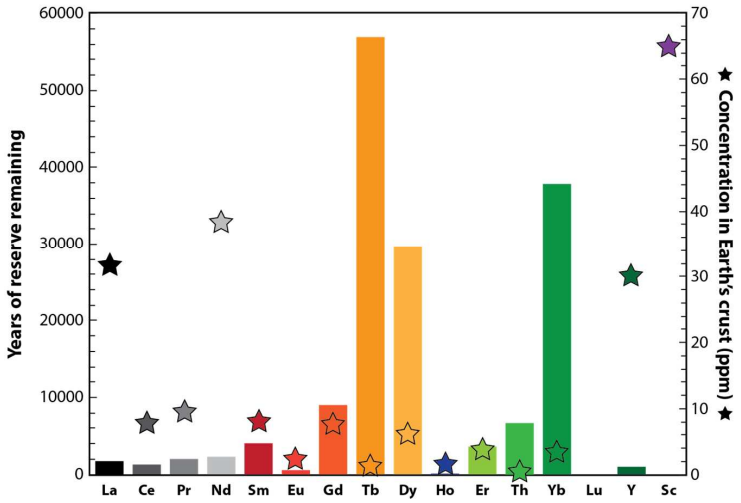

Figure 1. Estimated reserves of selected rare-earth elements (REEs: *x*-axis) in years (shown on left hand *y*-axis) and their abundance in the Earth's crust (right hand *y*-axis). The colored bar represents the number of years that element has left as a reserve. The corresponding star symbol illustrates the concentration of that element in the Earth's crust (ppm). Data from [4].

Most critical are the reserves of Europium (Eu), the only rare earth metal to have <1000 years remaining as a resource. It is used daily, in conjunction with phosphors, to generate red in televisions which use cathode ray tubes, and is a common component in compact fluorescent bulbs [8]. Also from Figure 1, lanthanum (La, which is three times more abundant than lead (Pb) in Earth's crust; [8]), Ce, praseodymium (Pr), neodymium (Nd), holmium (Ho), and yttrium (Y) all have reserves <2500 years. Respectively, these elements are used in mischmetal for spark effects in movies (La), in the oxide form as an abrasive for polishing glass (Ce); generating the green color in fake cubic-zirconia peridot (Pr), in high power magnets (Nd), in magnetic resonance imaging (MRI) machines to concentrate

the magnetic field (Ho), and in barium copper oxide powders for use in superconductors (Y; [8]). Figure 2 summarizes the short term (within 5 years), and medium term (5–15 years), criticality of REEs (in addition to cobalt (Co), gallium (Ga) indium (In), lithium (Li), and tellurium (Te)).

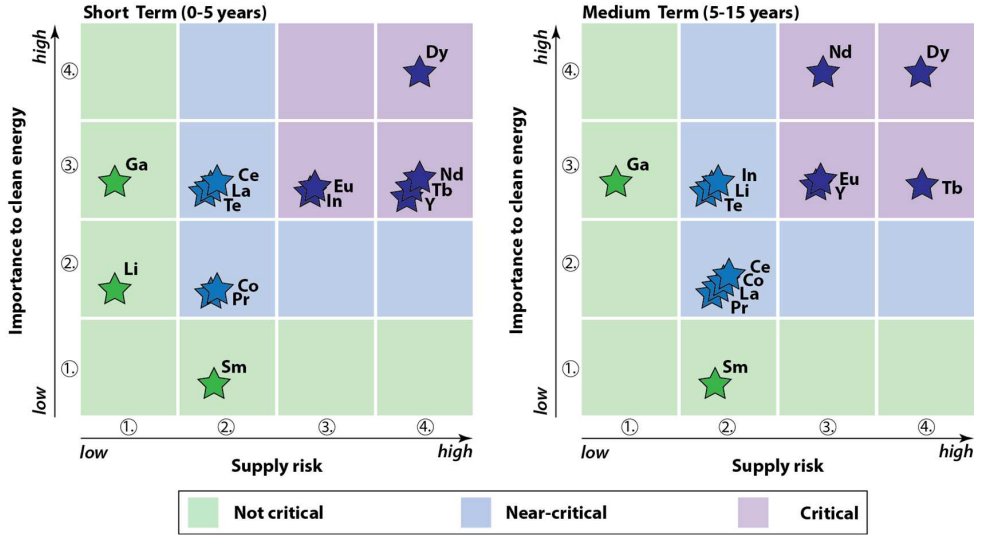

Figure 2. Figure modified from the United States Department of Energy [9] highlighting the criticality of rare-earth metals, starting in 2015. The star symbols for each element are colored to correspond with the criticality index in the legend. Note that the REEs, particularly dysprosium (Dy), Eu, Nd, terbium (Tb), and Y, are associated with both a high supply risk, and are considered highly valuable to clean energy within the next 13 years.

The following elements are both highly valuable to clean energy, and are experiencing a high supply risk, both in the short term, and medium term: Dy, Eu, Nd, Tb, and Y. Of all the elements shown in Figure 2, Li is the only element to change from a lower criticality index (not critical), to a higher criticality index (near critical). This change is associated with the projected increase in the use of lithium-ion batteries in vehicles (and hence an increased importance to clean energy; U.S. Department of Energy (DOE) [9]). As noted in the DOE report, market dynamics and increased research and investment in alternatives will ultimately contribute to the criticality of these elements in the future.

2. The Criticality of REEs in Our Society

The REEs have thus emerged as a critical materials group over the past 20 years and the uses, market demands, and holders of these materials have played integral roles in the growth of the global economy over this time period [10]. Specifically, REEs are deemed critical to the growing global green economy [9]. Generally, the demand for REEs ultimately relates to the unique orbital structures and transitions of electrons in orbitals of the REEs such as transitions involving intra-4f or 4f-5d that produce fluorescent light emissions, oxidation state changes in reactions or the magnetic properties of REEs. In a 2011 USGS report, REE applications market sectors were classified as metallurgy neodymium–iron–boron magnets catalysts glass including polishing and additives and other uses and detailed consumption in these areas are based on available reviewed 2008 data [11]. These general resource sectors have permeated nearly every aspect of the global economy with a wide variety of uses.

The REEs are also a critical material in clean energy technologies and within major areas of utility including wind turbines, lighting, magnets, and vehicles [9]. Several industry sectors are heavily dependent on the REEs owing to their magnetic, electrical, and optical properties. These industry sectors include but are not limited to defense, power generation, energy efficiency, catalysis, medicine [10].

The advent of REE based magnets in the 1960s revolutionized the utility of wind power [12]. Wind turbines utilize REE magnets in their dynamos. The REEs functionally provide stronger magnetic field in smaller volumes compared to their traditional Fe-based counterparts [12]. Thus, wind turbines have become an increasing important renewable energy source in the last 10 years and this technological evolution has been directly driven by REEs [9].

In addition, the REEs are used in a multitude of defense technologies in the US and are considered a strategic resource. Examples of some specific defense uses of REEs include motors for disk drives in numerous aircraft, land vehicles and command and control facilities, optical technologies including laser weapon detections and countermeasures and other equipment, satellite communications, radar and sonar components, as well as other technologies [13]. The REEs are also well recognized catalysts. For example, Ce is well recognized as an oxidative catalyst [14,15] and Eu has been used as a catalyst in molecular synthesis [16,17]. This is an area of use that is expected to grow as catalysis is directly tied to energy efficiency [9].

In a recent review, luminescence, medical imaging, and therapeutic applications were highlighted as the most important microcrystal and nanocrystal application areas [18]. In the context of medical technology, optical imaging, X-ray tomography (CT), positron emission tomography (PET) and magnetic resonance imaging (MRI) techniques (as stated earlier) can be enhanced by use of REE nanoparticles typically involving Dy, Gd, Tb, and Eu [18]. REE nanoparticles have also been investigated and used in the treatment of cancer in photodynamic therapies and photothermal therapies, in addition to the simple delivery of chemotherapy components [18].

All of the above uses are dependent on essentially mined resources. Recycling of REEs is challenging and not practiced widely [11]. What recycling does occur is primarily from fluorescent lamps, batteries, and magnets but is of limited scope, estimated at perhaps only 250 tons [19]. Identifying new REE resources, whilst continuing to improve and expand recycling efforts, is an absolute requirement for the continued utilization of REEs in the modern consumer economy and the emerging global green economy.

The Earth's population is projected to reach 8.5 billion by 2030 [20] yet the mining industry is currently downsizing [21]. This temporary decline is predominantly associated with quotas that are being placed on REE exportation, and a reduction of illegal mining operations by the Chinese government [4]. However, material and energy resources on Earth are ultimately limited hence sustaining our reliance on raw materials will likely require investment in, and utilization of, extraterrestrial resources. A first natural (and logical) step is the investigation and exploitation of resources on our Moon [22].

3. Earth's Moon: Missions to Our Nearest Neighbor

Study of Earth's Moon began several centuries ago in 1609 as Galileo made the first telescopic observations of Earth's nearest neighbor in space [23]. Observations, exploration, and the study of Moon formation and evolution have continued ever since the first spacecraft landed on the lunar surface in 1959 as part of the Soviet Union's Space Program (Luna 2). The most recent lunar landing occurred in 2013 through the China National Space Administration (the Chang'e 3 mission) and a follow-up mission, Chang'e 5, is scheduled to be launched November 2017. This will be the first lunar sample return mission since 1976 (Luna 24).

The sources of raw materials, on which the human race depends, have to date originated from one planet, Earth. Advances in space exploration technology however have the potential to expand our "closed planetary economy" to include extraterrestrial resources [24]. Efforts to map and characterize the lunar surface have been extensive, and are ongoing: SMART-1 (European Space Agency, 2004); Kaguya (Japan, 2007); Chang'e-1 (China, 2007); Chandrayaan-1 (India, 2008); Lunar Reconnaissance Orbiter (LRO, United States of America, 2009); Chang'e-2 (China, 2010); the Gravity Recovery and Interior Laboratory (GRAIL, United States of America, 2012); and Chang'e-3 (which included a lander and rover, the first lunar landing since 1976, China, 2013). Yet, not since the mission of

the Luna 24 mission in August 1976, has a spacecraft designed for sample return landed on the Moon, and not since December 1972 has humankind set foot on the lunar surface (Apollo 17) [25]. The Earth's Moon has previously been described as an "Earth-orbiting Space Station" [26] on which exist, natural resources that have the potential to be practically, and sustainably, used by humanity. The Earth's Moon is fundamental to advancing our understanding of the evolution of terrestrial planets and is the only other Solar System object for which a rich data set of geology, mineralogy, petrology, geochemistry, geochronology, and internal architecture exists. The exploration of the Moon and its resources is a fundamental step in furthering the exploration of our Solar System [26,27]. The potential use of Earth's Moon as a resource is thus an important discussion to have within the context of sustaining human society and the planning of future space investigations. If humankind is to one day live on extraterrestrial bodies, such as the Moon or Mars, then the dependency on Earth as a resource source needs to be minimized, and the development of in situ resource dependency maximized [28]. The establishment of a base station on the lunar surface may one day be required in order to facilitate humankinds' exploration of our Solar System to, and beyond, to Mars. This would require a self-sufficient operational base where fundamental life support materials existed, fuel components were available, and construction materials were accessible (e.g., [29–31]).

A decade ago, 14 space agencies developed a vision for human space exploration and established a network through which this could be communicated, and ultimately achieved [32]. This is The Global Exploration Strategy: The Framework for Coordination. The first target is the nearest one in our Solar System, the Earth's Moon. The Earth's Moon has been the focus of geoscientific and cosmoscientific investigations for decades. It is a window into early Solar System processes which were fundamental to the geological and chemical evolution of Earth, and it provides insights into the evolution of planetary bodies (e.g., [33–59]).

Numerous scientific, technological, socio-economical, and political rationales exist that justify our study and exploration of Earth's nearest neighbor in space, but in order to maximize the potential of the Moon as a resource, stakeholders and nations will have to effectively and sustainably collaborate [22]. In September of 2007, at the Wired Nextfest in Los Angeles, the Google Lunar XPRIZE (GLXP) was announced. This space competition, organized by XPRIZE is sponsored by Google, and offers $30 million USD in funding to privately funded teams who land a robot on the lunar surface. At the time of writing, four teams remain, each of which have secured launch contracts. These include: Moon Express (USA, launch contract with Rocket Lab); Synergy Moon (International, launch contract with Interorbital Systems); Hakuto (Japan, launch contract with the Indian Space Research Organization (ISRO)); and Team Indus (India, launch contract with ISRO). The prize is awarded for (1) successfully placing a spacecraft on the surface of the Moon; (2) traveling 500 meters across the lunar surface; and (3) transmitting high-definition images and video feed back to Earth [60]. Each team is scheduled to launch by the end of 2017. Not since 1976 has a spacecraft landed on the Moon. This year, that is scheduled to change several times over with the success of the above missions in addition to the November Chang'e-5 launch. The USA team, Moon Express is to date, the only company to publicly announce that they aim to mine REEs on the Moon. Moon Express proposes to construct a lunar railroad on "Earth's eighth continent", process ores using robots, and return the extracted elements back to Earth [61]. Prior to this, they must claim the Google Lunar XPRIZE. Only "then the second or third mission can involve bringing things back from the Moon" (Naveen Jain, co-founder and CEO of Moon Express, speaking to Susan Caminiti of CNBC in 2014 [62]).

In addition, the current Lunar CATALYST (Cargo Transportation and Landing by Soft Touchdown) initiative, managed by NASAs Human Exploration and Operations Mission Directorate, is collaborating with three commercial companies in order to develop technologies that could be used to transport materials to the lunar surface (https://www.nasa.gov/lunarcatalyst/). Through partnerships with Astrobotic Technologies, Masten Space Systems, and Moon Express, these collaborative efforts aim to result in the successful landing of commercial robotic spacecrafts on the Moon with "resource prospecting" being one of the capabilities that would be supported. As of 2017, NASA had issued a

second Request for Information regarding the "availability of small payloads that could be delivered to the Moon as early as the 2017–2020 timeframe" (https://www.fbo.gov/index?s=opportunity&mode=form&id=cbcd56e6afbd7dfad1ef9cd0fb52b6f7&tab=core&tabmode=list).

From past, present, and future remote sensing missions, to Apollo and Luna missions of the 1960s and 1970s, to the future plans for robotic landers on the lunar surface, there is no doubt of the interest and investment being placed on the exploration and potential utilization of our nearest neighbor in space.

4. Lunar Differentiation

4.1. The Lunar Magma Ocean

Today, the Moon is a differentiated planetary object with a core, mantle, and crust (Figure 3a). The present day internal architecture of the Moon has been constrained to: an upper mantle from 60 to 400 km; a mantle transition zone from 400 to 800 km; a lower mantle from to (at least) 1100 km; a fluid outer core (350 km radius); and a solid inner core (160 km radius, Figure 3a: [63–65]). In the absence of plate tectonics, the lunar crust and mantle have remained physically separate for the past ~4 billion years [64,66]. In order to better evaluate potential lunar resources, the geochemical differentiation processes associated with lunar formation and evolution need to be understood [67].

Fundamental to recent interpretations of lunar evolution, is the Lunar Magma Ocean (LMO) model. Following formation of the Moon, *c*. 70–110 Myrs after the onset of Solar System formation through a giant impact between proto-Earth and an impacting body (Mars-sized Theia), molten material rapidly accumulated and began to solidify [33–35,68]. Previous studies have investigated the extent to which the Moon was initially molten with models ranging from scenarios in which the initial LMO depth was as shallow as 400 km [41], molten to 1000 km [69], to a scenario where the whole Moon was initially molten [50].

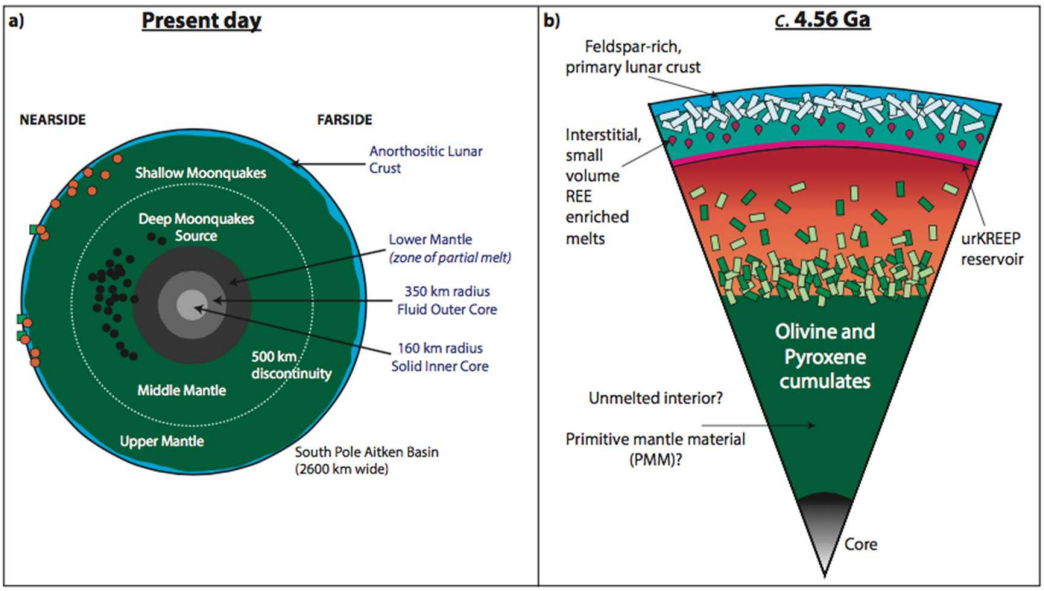

Figure 3. (**a**) Schematic cross section of the lunar interior (modified from [64,70]). Results from the GRAIL mission reveal an average crustal thickness of between 34 and 43 km, with impact basins exhibiting thicknesses near 0 km (the Moscoviense and Crisium basins [71]). The Moon's largest and oldest basin is the ~13 km deep South Pole Aitken Basin located on the lunar far side. From GRAIL, crustal thicknesses here are estimated at <5 km [71,72]. Moonquakes have been detected at both shallow (50–220 km) and deep (800–1000 km) depths within the lunar mantle. Seismic velocities have identified a distinct discontinuity at ~500 km, which has been associated with a phase change from spinel to garnet

(300–500 km, e.g., [73]). One hypothesis has been that this ~500 km discontinuity represents the extent of the mare basalt mantle source region; (**b**) Schematic summary of the LMO model showing dense settling out of early formed olivine and pyroxene. These cumulates sink to the lunar interior and form the source regions to the younger mare basalts. Following ~75–80% LMO crystallization, Ca-rich plagioclase feldspar is a liquidus phase, and being less dense than the surrounding mantle, forms an anorthitic flotation crust. Following ~99% solidification, the ITEs are concentrated in the last remaining dregs of the LMO and form the urKREEP reservoir from which KREEP-like signatures are inferred to originate. The depth to which an LMO on a primordial Moon existed has been debated for decades (whole Moon vs. partial Moon melting). For a summary of previous models, see [70].

The presence of magma oceans (or magmaspheres) on early formed planetary bodies has been debated and widely discussed throughout the planetary science community for decades [39,41,51,74]. The concept of a MO on an early formed Moon has established the context in which the geochemical and geochronological history of Earth's nearest neighbor in space is evaluated today. Simply, the widely-accepted sequence for crystallization of the LMO is the following: olivine → orthopyroxene ± olivine → olivine → clinopyroxene ± plagioclase → clinopyroxene + plagioclase → clinopyroxene + plagioclase + ilmenite [75]. As a young Moon solidified, the first phases to fractionally crystallize out (olivine and pyroxene, ± Fe-Ti oxides) were denser than the surrounding magma and sank towards the lunar interior (Figure 3b). Following ~75–80% solidification, low-density plagioclase feldspar became a liquidus phase and buoyantly rose to form an anorthitic feldspathic flotation crust (Figure 3b). This sequence of differentiation events accounts for the old anorthositic lunar highlands samples (*c*. 4.57–4.34 Ga; summary of ages presented in [55]), which have been interpreted as representing primary plagioclase-rich flotation crust, and the younger mare basalts (the majority at *c*. 4.0–2.0 Ga: [76], with a recent study suggesting magmatism may have occurred as recently as ~100 Ma: [77]), which were derived from source reservoirs in the lunar interior which had experienced previous melt (plagioclase) extraction (olivine and pyroxene cumulates, Figure 3b). This petrogenetic model for the anorthositic lunar highlands, and mare basalts, is further supported by the positive europium anomalies in the lunar highlands samples, complementary negative europium anomalies in the mare basalts, and the absence of plagioclase on the mare basalt liquidus [78–84].

At ~99% solid (e.g., [51,69,85,86]), the remaining LMO liquids would have been relatively enriched in incompatible trace elements (ITEs), as these elements are not easily incorporated into the crystal structures of the major silicate phases: olivine, pyroxene (±Fe-Ti oxides), and plagioclase feldspar. These elements would have included potassium (K), the REEs, and phosphorous (P, collectively referred to as "KREEP": Figure 3b) and are hypothesized to have formed a late-stage reservoir between the solidifying lunar mantle and crust. This reservoir, a residuum from LMO differentiation, is referred to as urKREEP, with the Germanic prefix "ur" meaning primeval [85]. The source of KREEP signatures in lunar rocks has thus been associated with an urKREEP origin.

It is noted here that there is currently debate regarding both the timing, and the duration, of LMO crystallization. Ages of lunar crustal rocks characterized by high proportions of anorthitic feldspar, and thus interpreted as representing primary lunar crust, range from 4.57 to 4.36 Ga ([87,88] for a review see [55]) while models of solidification range from 10 to 200 Myrs depending on whether tidal eating is invoked ([69,89] respectively). Ages associated with formation of the KREEP reservoir range from 4.48 Ga (from Apollo 14 zircons) [90] to 4.36 Ga (Lu-Hf isotopic systematics on KREEP basalts) [91].

4.2. Lunar Mineralogy

Mineralogically, the Moon is very simple with only four major phases: olivine ($(Mg,Fe)_2SiO_4$); pyroxene ($(Ca,Mg,Fe)_2Si_2O_6$); plagioclase ($Ca_2Al_2Si_2O_8$); and ilmenite ($FeTiO_3$) [42,92,93]. These phases dominate the Moon's major lithologies, the anorthositic lunar highlands, and the mare basalts (Figure 4). Figure 4a shows the lunar nearside with the location of the six Apollo landing sites also shown, note that Apollo 16 was the only mission which targeted the lunar highlands. The other

missions targeted various regions of the lunar maria. Figure 4b shows a characteristic lunar highlands sample, 60025, dominated by plagioclase feldspar. Figure 4c shows a typical mare basalt, characterized by pyroxene, plagioclase, ilmenite, and olivine. This particular sample is highly vesiculated and has been determined to originate from depths >250 km in the lunar mantle [94].

Minor phases also present throughout the lunar (Apollo, Luna, and meteorite) sample collection include apatite ($Ca_5(PO_4)(F,Cl)$); baddeleyite (ZrO_2); chromite-ulvöspinel ($FeCr_2O_4$-Fe_2TiO_4); iron (Fe(Ni,Co)); k-feldspar ($(K,Ba)AlSi_3O_8$); merrillite ($(Ca_3)(PO_4)_2$); pleonaste ($(Fe,Mg)(Al,Cr)_2O_4$); rutile (TiO_2); silica (SiO_2); ternary feldspar ($(Ca,Na,K)AlSi_3O_8$); troilite (FeS); zircon ($ZrSiO_4$); and zirkelite-zirconolite ($(Ca,Fe)(Zr,Y,Ti)_2O_7$) [93]. Several other minerals enriched in refractory elements, are also found on the Moon (some uniquely), including: dysanalyte $(Ca,Fe)(Ti,REE)O_3$, thorite ($ThSiO_4$); titanite ($CaTiSiO_5$); tranquillityite ($Fe_8(Zr,Y)Ti_3Si_3O_{24}$); yittrobetafite $(Ca,Y,U,Th,Pb,REE)_2(Ti,Nb)_2O_7$); zirconolite ($CaZrTi_2O_7$); and zirkelite ($(Ca,Th,Ce)Zr(Ti,Nb)_2O_7$) [95,96].

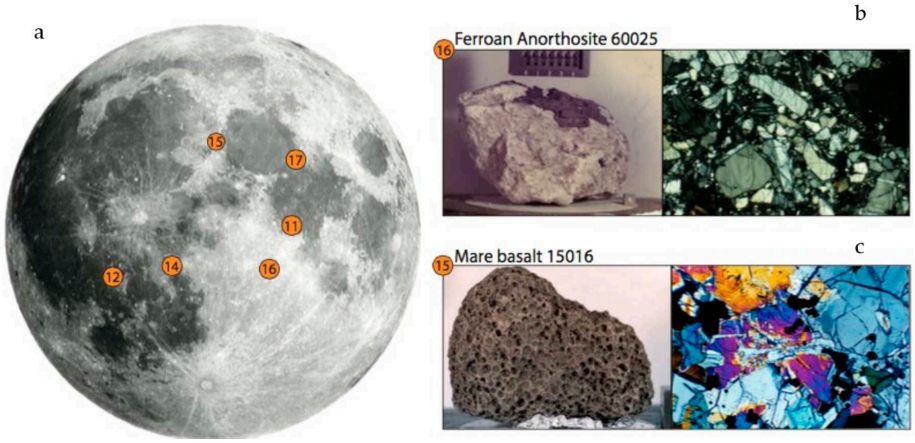

Figure 4. (**a**) Near side of the Earth's Moon with Apollo landing sites shown. The majority of landing sites targeted the lunar mare (dark regions); (**b**) Left hand image shows a hand sample of 60025, a Ferroan Anorthosite. Right hand image shows a thin section photomicrograph of 60025, characterized by 70–98% plagioclase feldspar [85,97,98]. (**c**) Left hand image shows a hand sample of 15016, a vesiculated olivine-normative basalt. Right hand image shows a thin section photomicrograph of 15016, characterized by olivine (6–10%), pyroxene (59–67%), plagioclase (21–27%), ilmenite (6%), and <1% total of chromite, ulvösplniel, and mesostasis [99–101]. All images are available from the NASA Lunar Sample Atlas [102].

5. Lunar Resources

5.1. The KREEP Source

Following study of the returned Apollo samples, an easily identifiable, and geochemically distinguishable, component within the lunar sample collection was apparent. This unique signature is associated with elevated REE, K and P (or, KREEP) [102]. Historically, the origin of the KREEP component in lunar lithologies has been debated with two principal theories regarding its petrogenesis proposed throughout the literature: (1) Partial melting of the solidified lunar interior following LMO crystallization and (2) extreme fractional crystallization of the primordial LMO (Figure 3b). In [103], partial melting was concluded as not being responsible for the observed abundances of ITEs in the KREEP-rich lithologies. This was due to inconsistencies in the behavior of elements in partial melting models, most notably the large fractionations between La and Lu (which is not observed). Instead, covariation of ~20 ITEs which cover a 10-fold range of abundances in samples which are derived from spatially distinct sample sites throughout the Apollo collection, further support their derivation from a common lunar geochemical reservoir ([103]; Figure 3b). The uniformity in ITE enrichment, consistent LREE/HREE ratios (light rare-earth elements/heavy rare-earth elements), and similarity

in $^{143}Nd/^{144}Nd$ isotopic signatures is therefore inconsistent with local-scale partial melting and subsequent fractional crystallization, but consistent with derivation from a reservoir formed during LMO differentiation (urKREEP) [104].

Today, KREEP-rich lithologies are demonstrably associated with relative enrichments in thorium (Th) and uranium (U) (Figure 5).

Evaluation of the distribution of KREEP-rich lithologies is therefore possible through gamma ray mapping [105,106]. Results from the gamma ray spectrometer onboard the orbiting Lunar Prospector orbiting spacecraft revealed a concentrated distribution of Th(and KREEP)-rich lithologies in the northern hemisphere of the near-side of the Moon (Figure 5). This distribution is also associated with the region known as Oceanus Procellarum, and the Imbrium Basin, and is now widely referred to as the Procellarum KREEP Terrain (or the PKT) [107]. The concentration of KREEP-rich lithologies on the near-side of the Moon in the PKT (Figure 5b) is not only associated with late stage LMO crystallization, but also later exhumation following an impact which formed the Imbrium Basin during a period of intense bombardment during the Moon's early history.

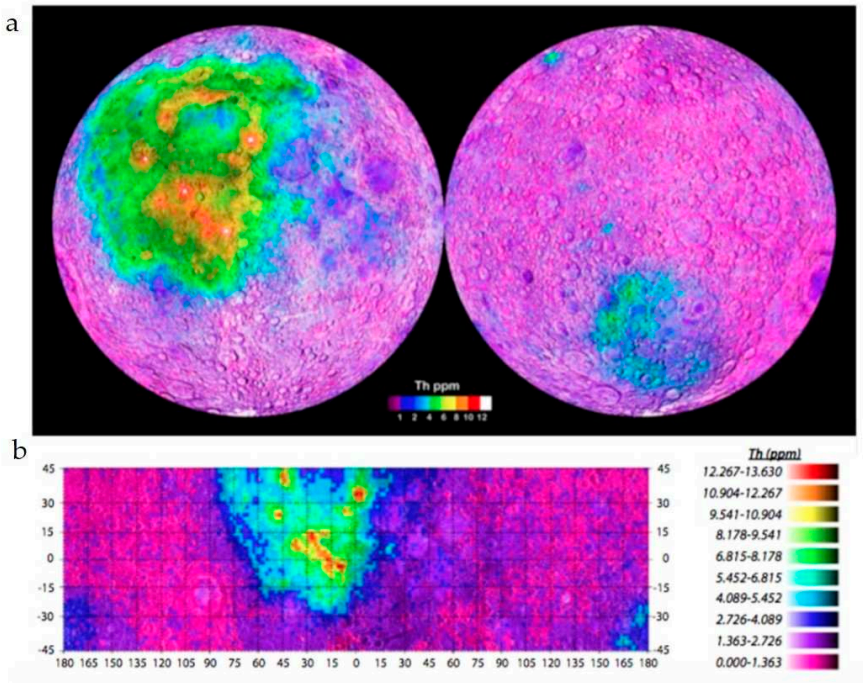

Figure 5. (**a**) From NASA, Thorium (Th) distribution map of the lunar nearside (left) and far side (right), mapped by the Lunar Prospector. Image available at [108] and used with permission; (**b**) Gamma ray spectrometer (GRS) generated map of thorium abundances for mid-latitudes with abundances >12 ppm in isolated locations. Modified from [105].

The volume of KREEP lithologies underlying Oceanus Procellarum has been estimated at 2.2×10^8 km^3, based on the concentration of radioactive (heat-producing) elements and the area mapped as "high-Th" (Figure 3a, [109–111]). From [109], potential REE reserves in these underlying KREEP rocks has been estimated at ~2.25×10^{14}–4.5×10^{14} kg.

5.2. Lunar REE-Bearing Minerals

The presence of KREEP components in lunar samples is "unequivocally accepted" yet a pristine urKREEP signature has not yet been found [112]. The composition of urKREEP, from which KREEP-rich lithologies derive their KREEPy signatures, was modelled in [112,113]. Figure 6 summarizes the primitive mantle-normalized REE-signatures of (1) chondrite; (2) different geochemical reservoirs on Earth: upper, middle, lower, and bulk continental crust; (3) the REE-signatures of lunar highland

samples (FANs), mare basalts, a lunar granite, a lunar dunite, and KREEP-rich lithologies; (4) signatures of REE-bearing phases found on the Moon so far (and discussed in more detail later); and (5) the signature of the urKREEP reservoir. As illustrated in Figure 6, and discussed earlier, the lunar highlands samples and mare basalts display complementary geochemical signatures with positive and negative Eu-anomalies respectively.

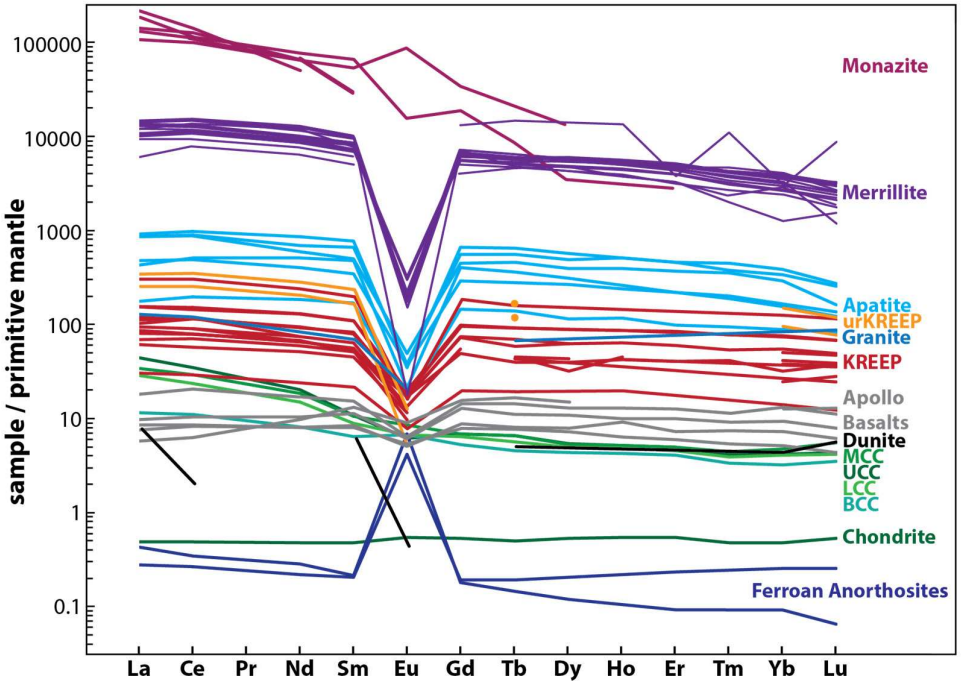

Figure 6. Rare-earth elements—Earth's primitive mantle normalized concentrations of terrestrial and lunar reservoirs, rocks types, and REE-bearing phases. Samples and data sources (all lunar data is available in the Lunar Sample Compendium [94] unless stated otherwise): Ferroan Anorthosites 60025 and 62236; Chondrite: [114]; Dunite: [115]; BCC (Bulk), LCC (Lower), MCC (Middle), and UCC (Upper Continental Crust) from [116]; Apollo Basalts: 12011, 12075, 14053, 15016, and 70017; KREEP basalts 12013, 14073, 14076, 14078, 14303, 14310, 15382, 15386, 15405, 61156, and 72275; Granite: [117]; urKREEP from [112]; Apatite and Merrilite from [118]; and Monazite from [119].

From [112,113] the degree of fractionation that would be required to form a residual liquid during LMO that has the composition of urKREEP is "within the realm" of silicate liquid immiscibility, whereby two melts—one K-rich and one REEP-rich—are segregated. This process has the potential to account for the presence of lunar granites (derived from the K-rich melt) and evolved phosphate phases in highland samples (see discussion later). The KREEP-rich fraction then has the potential to ascend and interact with the lunar crust, potentially acting as a metsomatic agent. As shown in Figure 6, the modeled composition of urKREEP (orange) is elevated in KREEP components relative to the KREEP-like signatures (shown in red), and is higher in KREEP components than any other lunar lithology (Granite, Apollo Basalts, Dunite and the FANs).

The majority of the ITEs on the lunar surface, in rocks and soils, are associated with the PKT (Figure 5). However, the majority of lunar samples contain apatite and/or merrillite as a trace phase (Figure 6), and in samples which exhibit a KREEP signature, merrillite (H-free whitlockite) is almost always present, often co-existing with apatite [120]. Figure 7a–c shows several excellent examples of lunar fluorapatite in an Apollo 10 basalt, and lunar apatite crystals lining vugs in the Apollo 14 breccias. In both examples, (fluroro)apatite occurs as euhedral to subhedral grains.

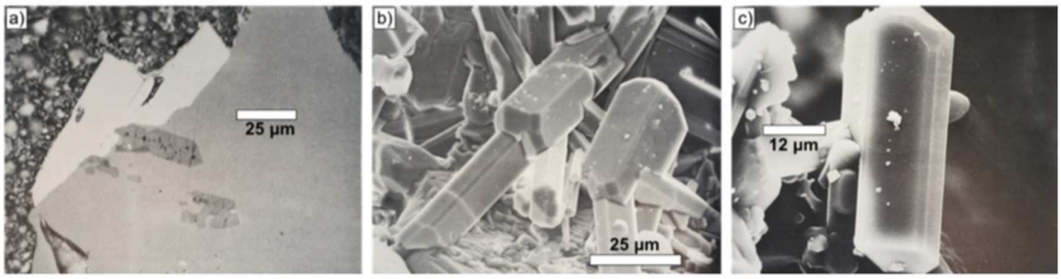

Figure 7. (**a**) SEM photograph of Apollo 10 basalt (10047): fluorapatite in pyroxferrite, in contact with ilmenite. Upper left portion is epoxy; (**b**) SEM photograph of apatite crystal in Apollo 14 breccia vug; (**c**) SEM photograph of doubly terminated apatite crystal in Apollo 14 breccia vug. All images from [95].

Also shown in Figure 6 are normalized REE compositions of REE-bearing phases found throughout the lunar sample collection: apatite, merrillite, and monazite. In lunar merrillite, REE substitutes for Ca, and H is substituted by Na and K. This mineral appears to be unique to the PKT with the formula $Ca_{17.3}Y_{0.4}(La\text{-}Lu)_{0.88}(Mg,Mn,Fe)_{2.4}(Na,K)_{0.07}(P,Al,Si)_{13.9}O_{56}$ (sample 14310,123; [96]). While significant proportions of the KREEP REE budget are associated with merrillite, which can constitute up to 3% of a lithologies volume in the PKT, the amount of merrillite is unfortunately too small for economical extraction of metals on the Moon based on current understanding [96]. This of course does not rule out the discovery of future, more concentrated, deposits.

From [121] Apollo 14 Quartz (whitlockite (merrillite) rich) Monzodiorite fragments (2–4 mm) in lunar soil has the highest REE concentrations of any lunar material reported to date (excluding merrillite separates). One 18.4-mg merrillite-rich particle (W-QMD 14161,7373) was found to contain 11% phosphates and 1% zircon. This particle exhibited a REE normalized pattern that resembled KREEP, but with a distinctly higher La/Yb ratio (4.78 vs. 3.38 (from 15386)), consistent with the presence of merrillite. The petrogenesis of this highly enriched REE sample was reconciled in a silicate-liquid immiscibility model after fractional crystallization involving merrilite. This model was also used to account for some of the observed geochemical trends in lunar granites [112,113,121]. KREEPy geochemical signatures are also present in impact melt breccias (IMBs) collected from the Apollo landing sites (most notably 14, 15, 16, and 17; [122]). These samples have an average (from each landing site) La (ppm) ranging from 21.2 to 87.4, Ce (ppm) from 55 to 224, Sm (ppm) from 9.92 to 38.5, and Lu (ppm) from 0.92 to 3.82 [122] but exhibit similar inter-element ratios: La/Lu: 22.8–23.0; Ce/Sm: 5.5–5.8; Ce/Lu: 58.6–59.8 which attest to their LREE enrichment.

One other REE-bearing lunar phase, which is present in lower abundance relative to merrillite and apatite, is monazite. Until 2006 monazite had only been identified as small (10 µm × 3 µm) inclusions in pyroxene from Apollo 11 basalts (sample 10047,68; Figure 6; [95]). Additional lunar monazites were reported in [119], where particles ~0.5–3 µm in size were identified in regolith from the Luna 24 samples. One striking feature of one of these newly identified monazites was the positive Eu-anomaly (Figure 6) and associated lack (below detection limit) of Th. This was attributed to crystallization from an aqueous solution during metasomatic alteration of Eu-rich plagioclase in primary mare basalts which contained REE-bearing phases (merrillite and apatite for example; [119]).

In addition to monazite, merrillite, and apatite, the REE-rich phase yittrobetafite has been found in sample 14321,1494 (a clast-rich, crystalline matrix breccia known as "Big Bertha") and contains 17.67 wt. % Nb_2O_3; 4.33 wt. % UO_2 (38,200 ppm U); 2.38 wt. % Nd_2O_3 (20,420 ppm Nd); 12.00 wt. % Y_2O_3 (94,500 ppm Y); and 12.81 wt. % REEs [123].

At the time of its identification in Apollo 11 and Apollo 12 basalts, the mineral tranquillityite was not only a new lunar silicate mineral, it was a new mineral. Initially, it was identified as "A" and as an "unnamed yttrium-zirconium silicate" in [124,125] respectively. It is associated with interstitial phases (e.g., troilite), and occurs as thin laths in coarse-grained cristobalite [126]. Geochemically, it is enriched

in Zr (12–13 wt. %), Y (1.0–4.6 wt. %), and Nd (0.1–0.25 wt. %), and was not discovered on Earth until 2011 (in Australia, [127]).

In order for a mineral deposit to be mined as an ore, the concentration of the desired element must be high enough for economic extraction, meaning that its initial abundance must also be high enough so that a differentiation process can concentrate it. While samples from the Apollo 14 and 15 collections exhibit REE concentrations higher than urKREEP (up to four times higher), their abundances are still low relative to terrestrial ores [24,42,128]. However, direct sampling of the high Th regions of the PKT (Figure 5), has not yet occurred and with the spatial resolution at ~10 s of km, the PKT has the potential to have higher REE concentrations at a local scale, hence future explorations may yet yield REE deposits that are viable for exploitation and extraction [24].

5.3. Other Potential Lunar Resources

The natural resources on the Moon can be classified into the following categories: rocks and minerals, soil (regolith), and fumaroles and vapor deposits [129]. All of these have the potential to be processed and utilized as metals, ceramics, and glass. Despite all the elements that are present on Earth being present on the Moon, several of Earth's widely used elements (such as copper, gold, and chlorine) are widely dispersed and, based on current understanding, not concentrated in viable deposits on the Moon [26]. Lunar resources have several broad uses, none of which are mutually exclusive (1) lunar exploration support (In-Situ Resource Utilization, or ISRU); (2) support of economic and inquiry-driven science in the near-Earth-Moon region of the Solar System; (3) contributions to Earth's global economy; and (4) provision of resources (including through recycling) in support of Mars missions [24,30,130–133].

Lunar resources that have gained significance, many of which have been previously presented and discussed in [24,26,133,134], are briefly summarized here.

5.3.1. Helium-3

Helium-3 has the potential to be used as a fuel for atomic fusion reactors [133]. In the absence of a magnetic field and an atmosphere, the lunar regolith has been successively implanted with solar wind particles (ions) for billions of years from which trapped H and He could be released. In this case, H could be used for rocket fuel, and ^{3}He as an energy source [24,26,135,136].

5.3.2. Water

Evidence (indirectly) for water at the lunar poles was provided by the Lunar Prospector, and later supported by the Lunar Crater Observation and Sensing Satellite mission which reported a concentration of 5.6 $\pm$ 2.9 wt. % (1σ) for water ice in lunar regolith [137–139]. Considering a water mass of 5.6 wt. %, and a density for the lunar regolith of 1660 kg/m^3, a potential 2900 million tonnes of water exists within the upper 1 m of regolith [24]. Based on current human consumption of 10 billion tonnes of freshwater per day (www.theworldcounts.com/stories/average-daily-water-usage), and 80–100 gallons of water use/person/day [140], 2900 million tonnes (of lunar freshwater) would sustain today's global population for 1 min and 12 s, and one individual for 20.1–26.2 billion years (based on current average use).

5.3.3. Oxygen

Oxygen could be sourced from lunar water, either from polar ice or hydrated regolith from pyroclastic deposits [24]. In addition to this, 20 different approaches exist for extracting oxygen from the lunar regolith (8 of which can be considered plausible, [141]). Oxygen could also be exploited from the more extensive lunar highlands, where anorthite is abundant ([142] Schwandt pers. comm. in [24]).

5.3.4. Aluminum

Aluminum (Al) is widely used throughout society today in fuselages of aircraft, food and beverage packing containers, packaging, kitchen utensils and beer kegs, to name but a few. It is the most abundant metal in Earth's crust (~8%) where it is mined from bauxite and cryolite ores. The lunar highlands are however comparatively enriched with between 10 and 18 wt % Al due to the abundance of anorthitic plagioclase feldspar, from which Al could be extracted [24,26,141].

5.3.5. Magnesium

Magnesium (Mg) is widely used in the manufacturing of race cars, airplanes, and bicycles (Grey, 2012). On the Moon, Mg is an abundant component of the lunar regolith, and certain lunar lithologies, predominantly in the form of MgO in olivine. Within the context of lunar exploration, it has the potential to be utilized in situ (ISRU) to form alloys and contribute to the manufacturing of a lunar base [143,144].

5.3.6. Iron

Historically, Iron (Fe) was a dominant component of the Industrial Revolution and since then has been widely utilized in the production of alloys (e.g., steel) due to the ease at which it can be tempered. Similar to to Mg, it is an essential component of the lunar regolith in the form of ilmenite (~10%) and as Fe particles [145] while the lunar crust contains ~3 wt % Fe [146]. Utilization of all metals (including Al and Mg) as an in-situ resource on the Moon is a "logical step" in the exploration of space [145].

5.3.7. Basaltic Glass

Basaltic glass, and in particular glass fibers, could be used as structural reinforcements in lunar concrete structures supporting the development other ISRU technologies [147–150].

5.3.8. Vacuum

From [133], telescopes placed on the lunar surface would experience a "lack of an attenuating atmosphere" while any metallic component would not rust. In addition, the lack of an atmosphere would also limit the distortion and attenuation of laser beam communication, and promote technological advancement, particularly in the production of glass from the regolith.

5.3.9. Lunar Regolith

The composition of the lunar regolith represents the results of billions of years of impacts [28,127,150–152]. This has been of specific interest due to its potential application as a construction or manufacturing material, as a chemical consumable, or as a propellant [24,153,154] and will likely provide the initial (and major) lunar resource [29]. More recently, lunar regolith has been proposed as a material that could be utilized in 3-D printing technology to build lunar infrastructure (e.g., [154]).

5.4. REEs beyond the Moon

The only other planet from which samples are known to have been derived from is Mars. Yet compared to Earth and the Moon, relatively little is known about the differentiation and geological evolution of the red planet (e.g., [155]). To date, there have been no sample return missions hence our understanding of Martian geology is based on the 107 meteorites (as of 1 August 2017, [156], and their associated pairs) that have survived passage through Earth's atmosphere. This number is considerably less than the 344 lunar meteorites identified so far, and their pairings (as of 1 August 2017, [157]) and the >1000 samples brought back by the Apollo missions (including rock samples and lunar regolith, [158]).

From the REE characteristics of martian meteorites, it has been shown that Mars differentiated very early in the history of the Solar System (~4.5 Ga) to form a metallic core, a silicate mantle, and a crust, and broadly differentiated to form a LREE-depleted reservoir (low La/Yb, high Sm/Nd) and an inferred, complementary LREE-enriched reservoir (high La/Yb, low Sm/Nd; [159]), the latter of which remains to be directly sampled (see discussion later; e.g., [160–167]). Unlike the lunar sample collection and the lunar magma ocean model (Figures 3 and 4), Mars lacks an Al-rich anorthositic crust. This observation is attributed to crystallization of garnet during Mars magma ocean crystallization (e.g., [159,165]). As Mars is larger than the Moon (~twice the diameter), higher pressure in the planet's interior would have promoted the crystallization of high pressure phases, such as garnet. This would have had a significant impact on the crystallization sequence of a magma ocean as garnet contains Aluminum. From experiments at pressures of 3–5 GPa, the following sequence for martian magma ocean crystallization has been proposed: olivine → olivine + orthopyroxene → orthopyroxene + clinopyroxene → clinopyroxene + garnet + ilmenite → clinopyroxene + garnet [168]. At higher pressures, the crystallization of garnet occurs earlier, but between the crystallization models is the consistent absence of plagioclase (see [168]). Following ~99.5% martian magma ocean crystallization, a late-stage liquid enriched in incompatible elements (including KREEP) has been modelled. The overall geochemical characteristics of this evolved reservoir are very similar to lunar KREEP [168].

As presented earlier within the context of the Moon, REE-bearing minerals are volumetrically rare in extraterrestrial samples. This can be in part attributed to the scarcity of felsic igneous rocks (as sampled to date) and the lack of high-temperature fluids which would concentrate these elements. With no sample return missions having yet been completed to Mars, mineralogical and chemical information is derived from (1) elemental surface maps obtained by Mars-orbiting satellites (e.g., the Gamma-Ray Spectrometer (GRS) on board Mars Odyssey); (2) landers and rovers on the martian surface (e.g., the Mariner missions, Mars 3, Viking 1, Viking 2, Pathfinder, Opportunity, Phoenix, and most recently Curiosity); and (3) meteorites.

Maps from the GRS instrument have summarized the distribution of chlorine, calcium, potassium, iron, silicon, and hydrogen across the martian surface, where like the Moon (Figure 5), thorium exhibits a high degree of correlation with potassium [169,170]. From these results, the martian surface has been shown to be broadly composed of basaltic material (iron, silicon, calcium), sulfur, chlorine, hydrogen, potassium, and thorium in addition to elements that were not mapped by the GRS (e.g., magnesium and sodium; [170]). More recent results from analyses of martian soil in Gale Crater by Curiosity's onboard instruments (ChemCam and APXS (Alpha Particle X-ray Spectrometer)) reveal a dominance of silicon, titanium, aluminum, iron, magnesium, calcium, and sodium. Other elements detected included potassium, chromium, manganese, phosphorus, sulfur and chlorine [171].

To date, only one of the meteorites—a polymict regolith breccia (sample NWA 7034) and its paired stones—is considered representative of the modern-day martian surface, with the other 106 Martian samples being igneous in nature (shergottites, orthopyroxenite, clinopyroxenite, dunite) and thus providing insights into the evolution of the Martian interior [156,172–175]. Figure 8a illustrates and summarizes the REE characteristics of these different classes of martian meteorites (including NWA 7034), along with the patterns of individual REE-bearing phases within NWA 7034 recently sampled by [176]. As shown, NWA 7034 exhibits LREE enrichment in comparison to other martian rock types with absolute concentrations of La and Lu of 13.7 and 4.3 ppm, respectively. Throughout the igneous lithologies, the enriched basaltic shergottite exhibits the highest concentrations of REEs with 4.4 ppm La, 8.4 ppm Nd, 4.7 ppm Gd, and 0.43 ppm Lu (sample NWA 7257) while the orthopyroxenite and the depleted olivine-phyric shergottite exhibit the lowest LREE abundances (La at 0.15 and 0.29 ppm respectively, Ce at 0.43 and 1.07 ppm respectively). The orthopyroxenite and dunite samples exhibit the lowest HREE abundances (0.255 and 0.11 ppm Yb respectively, and 0.037 and 0.015 ppm Lu respectively).

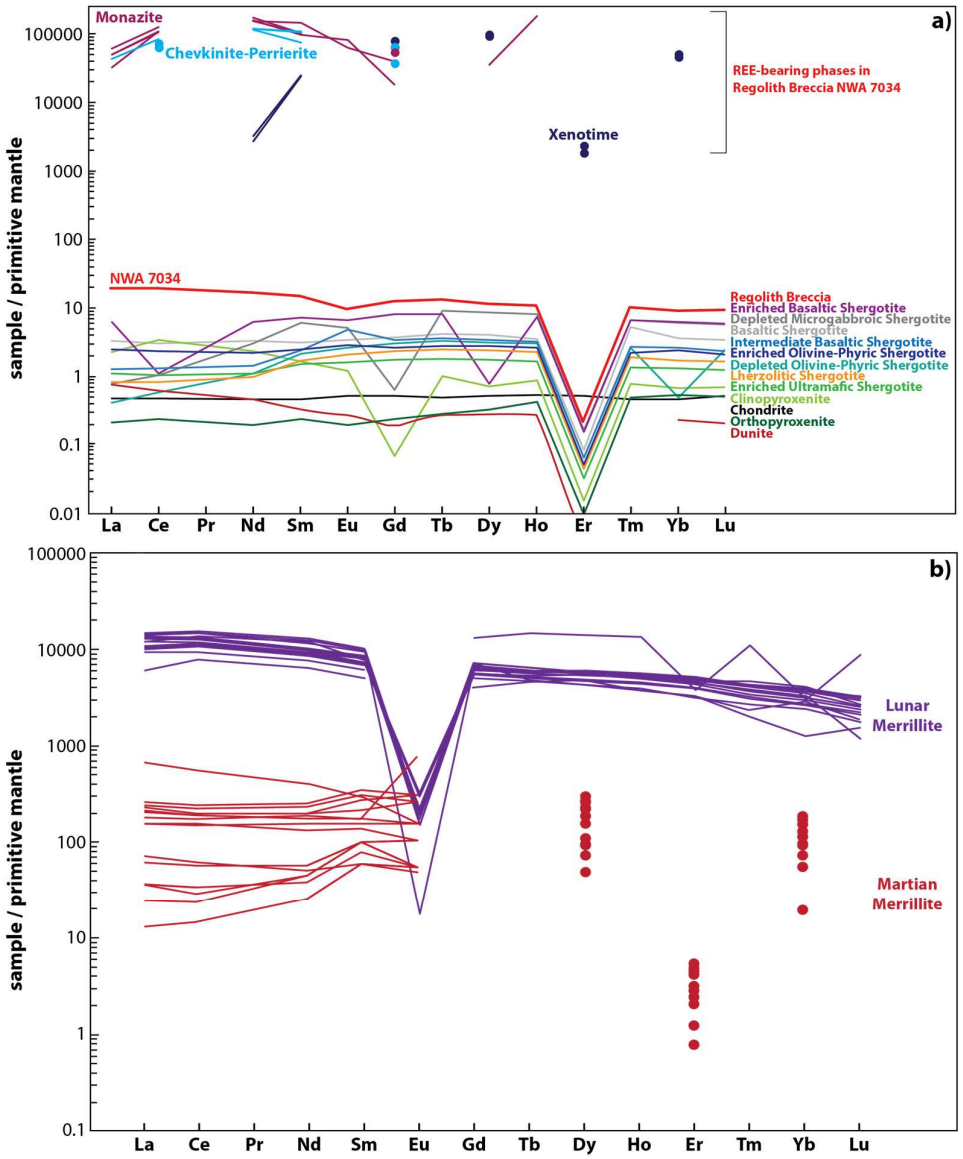

Figure 8. (**a**) Summary of the REE characteristics of martian samples including the recently discovered regolith breccia, NWA 7034 and its REE-bearing phases. All data is available through the Martian Meteorite Compendium [177]. NWA 7034 data from [176]; (**b**) Comparison of lunar and martian merrillite. Data sources: [116,178].

The most common REE-bearing phase throughout the martian meteorite collection is merrillite ($(Ca_3)(PO_4)_2$), a common accessory phases in extraterrestrial samples (as is apatite, see earlier discussion of the Moon). Throughout the martian sample collection, merrillite has been identified as the dominant host of the REEs [178]. Merrillite has been found in the shergottites (olivine-phyric, basaltic, lherzolitic), the orthopyroxenite, and the recently discovered regolith breccia (Figure 8a). As shown in Figure 8b, the abundances of the REEs in martian merrillites are significantly lower than in lunar merrillites. Broadly, the REEs substitute into the Ca site in the merrillite crystal structure, a substitution that is demonstrably more pronounced in lunar merrillites (Figure 8b). This observed difference is almost two orders of magnitude with respect to the LREEs (Figure 8b) and has been attributed to differences in their source melt composition, with the relatively depleted LREE patterns associated with derivation from depleted martian mantle sources [178], and the relatively enriched LREE patterns (La_N up to 699, where "$_N$" refers to the primitive-mantle normalized value) associated with LREE enrichment (e.g., [179]). This enrichment has been hypothesized to be associated with post martian

mantle differentiation, potentially as a result of small degrees of partial melting which concentrated a LREE component which was assimilated by a parental magma (e.g., [180,181]). Alternatively, this LREE component has been suggested to have been derived from the Martian crust (e.g., [182]) or a KREEP-like component associated with late-stage martian magma ocean crystallization and similar to that which has been identified in lunar samples (see earlier, e.g., Borg and [63,183]). While the origin of this LREE-enriched component remains poorly constrained (e.g., [184]), the differences between lunar and martian merrillites indicate that Mars experienced a different petrogenetic history than the Moon (Figure 8b; e.g., [120]).

Sample NWA 7034 (and two of its paired stones) have been reported by [176,185,186] as the first Martian rocks to contain apatite ($(Ca_5(PO_4)(F,Cl)$);-hosted monazite ($(LREE)PO_4$), monazite ($(LREE)PO_4$)-chevkinite-perrierite ($(Ce,La,Ca,Th)_4(Fe^{2+},Mg)_2(Ti,Fe^{3+})_3Si_4O_{22}$) in a clast, and coexisting chevkinite-perrierite respectively (Figure 8a). In the most recent study [176], xenotime and merrillite are also reported (Figure 8a). The major mineralogy of these martian surface rocks is characterized by alkali feldspar, plagioclase, pyroxene, with minor magnetite, pyrite, zircon, and phosphates [173–175] with the newly identified REE-bearing phases listed above all present at the sub-micrometer scale. From [176], monazite was found as inclusions in apatite and was proposed as having an origin associated with fluid-phosphate and fluid-rock interactions occurring at elevated temperatures on Mars, within the source rocks prior to their incorporation into the regolith breccia. These hydrothermal fluids were hypothesized to have originated from igneous intrusions intruding into the martian crust, or from impacts. This latter hypothesis presents a scenario in which REE-mineralization on Mars could be linked to impact cratering and thus presents craters as a potential location for REE- mineral resources on Mars [176].

Beyond samples from the Moon and Mars, other REE-bearing phases within other types of extraterrestrial materials are known. A summary of the REE characteristics of the most common type (broadly classified as stones, or stony-type) is shown in Figure 9.

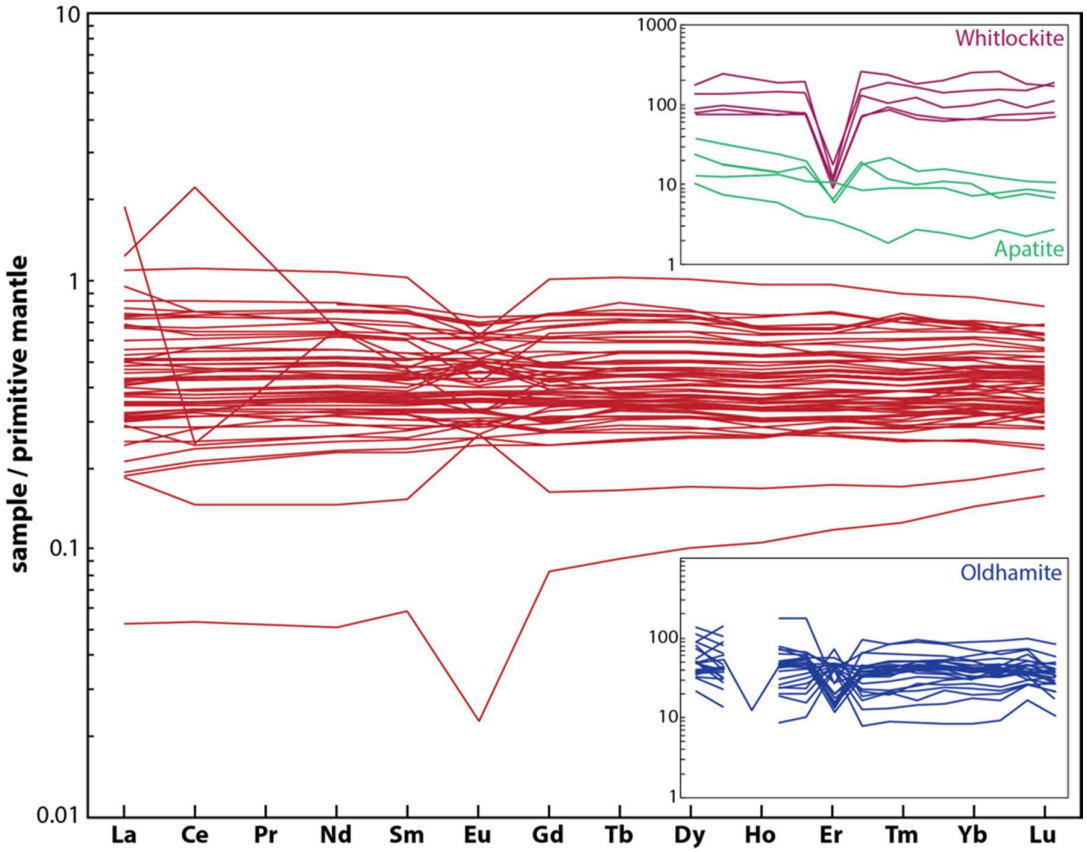

Figure 9. Summary of the REE characteristics of stony meteorites (chondrites types CI1, CM2, CO3, CV3, EH3, EH4, EH5, EL6, EH6/7, EL7, H4, H6, L4, L5, L6, LL4, LL5, and LL6, achondrite type: aubrite). Data source: [187]). Also shown are two inset graphs which illustrate the REE characteristics of several of the REE-bearing phases found within the stony meteorites. Results from oldhamite are shown in blue (data from from achondrite aubrite samples Bustee and Mayo Belwa, and two EL6 chondrite: Jajh deh Kot Lelu and Khairpur; [188]). Results from apatite and whitlockite are shown in green and purple, respectively (data from H4 chondrite Yamato-74371; [189]).

Of the 63 bulk rock primitive-mantle normalized REE signatures shown in Figure 9, 61 are chondrites (including samples from the following categories: CI1, CM2, CO3, CV3, EH3, EH4, EH5, EL6, EH6/7, EL7, H4, H6, L4, L5, L6, LL4, LL5, and LL6) and two are achondrites (classification: aubrite). The two aubrite samples represent the two most REE-depleted samples, consistent with their differentiated nature. As has been discussed within the context of lunar and martian samples, REEs are typically concentrated in minor phases. This is also the case with respect to the stony meteorites with sub-mm phosphates (e.g., apatite, whitlockite, and merrillite) and oldhamites ((Ca, Mg, Fe)S) being common carriers of the REEs (up to ~1600 ppm, or 0.16 wt. %). These phosphate phases are estimated to constitute ~0.6% of the whole rock sample [190] and their REE patterns are shown as insets in Figure 9. Broadly, these REE-bearing phases are enriched by 1–2 orders of magnitude in comparison to the bulk samples but do not extend to the same degree of enrichment as observed in lunar and martian minor phases (Figures 6 and 8).

As shown by the bulk stony meteorite data in Figure 9, little difference exists between the different types of chondrites. They exhibit low REE abundances and are therefore unlikely to represent a viable extraterrestrial REE resource. This is consistent with the findings of [191] who discussed the possibility of mining chondritic asteroid materials. While the REEs of these types of extraterrestrial materials are "not worth mining yet" and that the mining "makes little sense", due to their low abundances, [191] proposed they could be a potential platinum group element (PGE) resource. The PGEs include the

elements platinum (Pt), palladium (Pd), iridium (Ir) osmium (Os), rhodium (Rh), and ruthenium (Ru). These elements are of industrial significance with applications to the (petro)chemical and technological sectors. For example, Pt is widely used in the production of catalytic convertors and is combined with rhodium to produce an alloy utilized in fertilizers and explosives [192].

5.5. Missions beyond the Moon

Current plans to explore Mars include NASAs upcoming InSight (Interior Exploration using Seismic Investigations, Geodesy and Heat Transport) mission and the Mars 2020 rover. The InSight mission will place a lander on the Martian surface with a launch date of 5 May 2018, and a landing date of 26 November 2018 [193]. The objective of this mission is to explore the Martian interior. The Mars 2020 rover is scheduled to launch in July/August 2020 with a proposed landing in February 2021 [194]. One of the aims of this mission to prepare for human exploration of Mars which will in-part be achieved through extraction of oxygen from Mars' CO_2 rich (~96%) atmosphere. Current plans for human exploration of Mars through NASA missions are associated with sending humans to the red planet in the 2030s [195]. Associated with this goal is transport of equipment to cislunar space and the establishment of a "deep-space gateway". Phase 1 of this is scheduled between 2018 and 2026 and would include four crewed flights that would deliver key components of the Deep Space Transport vehicle to cislunar space ([195], see also [196]). At the time of writing, no known mission plans exist to mine Mars with the existence of ores on Mars (REE-dominated or not) "hypothetical" [197]. Alongside NASAs interest in the red planet, the European Space Agency (ESA), in collaboration with the Roscosmos State Corporation, is planning to send its ExoMars lander in 2020. In addition, several nongovernmental organizations also have plans to explore Mars with SpaceX planning to launch robotic capsules in 2018 and Mars One planning robotic missions in 2020, 2022, and 2024 [198].

In addition to current, upcoming, and proposed missions to the Moon and Mars (see earlier), in situ chemical characterization of other rocky objects in our Solar System through missions to Near Earth Asteroids (NEAs) aim to advance our understanding of the elemental composition of planetary materials. This approach to quantifying the geological and geochemical features of nearby objects was pioneered in 2001 through NASAs Near-Earth Asteroid (NEA) Rendezvous-Shoemaker mission to Eros, the second largest NEA [199]. More recently, the Hayabusa mission administered by the Japanese Space Program, JAXA (Japan Aeropsace Exploration Agency), landed on NEA 25143 Itokawa in 2005. This led to the return of regolith samples to Earth in 2010 [200]. A follow-up mission, Hayabusa 2, launched in 2014 to asteroid 162173 Ryugu. This mission is scheduled to land on the asteroids surface in 2018 prior to returning samples to Earth in 2020 [201]. More recently, 2016 saw the successful launch of OSIRIS-Rex (Origins-Spectral Interpretation-Resource Identification-Security Regolith Explorer) to the asteroid 101955 Bennu. This mission represents NASAs first attempt to return samples to Earth from a NEA [202].

Whether an extraterrestrial resource is identified as an (REE) ore deposit or water, or even something else, the resources first need to be evaluated, the technology associated with their mining and extraction demonstrated and validated, and successful extraction and application shown [28]. As presented here, there are extraterrestrial sources of REEs in the form of volumetrically minor phosphate phases in lunar, martian, and other meteoritic material. Despite there being little geological and geochemical evidence to support the notion that these REEs exist in concentrations where mining them would be justifiable [186,188] future explorations may change this [24]. It is likely that the future exploration of space will also be pursued for commercial reasons (Virgin Galactic as a current example) yet science stands to be a significant beneficiary of this endeavor [203].

6. Conclusions

Daily use of REEs by modern day society is placing an increasing demand for extraction of these elements from limited terrestrial resources. With an increasing population, a projected 8.5 billion by 2020, it is natural to consider exploration and characterization of extraterrestrial REE sources in

order to sustain our reliance on raw materials and energy reserves. Earth's nearest neighbor in space, the Moon, is a logical first target both in terms of evaluating resource potential.

Following formation of the Moon as the result of a giant impact between proto-Earth and an impacting Mars-sized body *c*. 70–100 Myrs after the onset of Solar System formation, molten material (a primordial magma ocean) began to solidify and differentiate. After ~99% crystallization a KREEP (potassium, rare-earth element, phosphorus)-rich layer concentrated incompatible elements, a geochemical signature detected in many lunar samples today. Today, KREEP-rich lithologies are associated with enrichments in thorium on the lunar near-side (in the PKT), as observed by the gamma ray spectrometer on the Lunar Prospector. The volume of KREEP-rich lithologies associated with this region of the Moon is estimated at 2.2×10^8 km^3, with potential reserves of REEs at ~2.25×10^{14}–4.5×10^{14} kg. The majority of lunar samples contain REE-bearing phases as minor or trace components, typically apatite and/or merrillite with KREEP-like lithologies almost always containing merrillite. The presence of merrillite has the potential to account for up to 3% of a lithologies volume in the PKT however, this does not permit the classification of REEs on the Moon as ores. While REE abundances of trace phases in lunar rocks are high, their abundances are low compared to terrestrial ores meaning there is to date, no geological evidence to support mining the Moon for REEs yet. With the development of future technologies capable of mapping at higher resolutions, and in situ exploration by future missions, economically viable lunar resources may yet be discovered. However, other potential resources do currently exist on the Moon—including helium-3, water, oxygen, and metals (Fe, Al, Mg)—which will likely be fundamental to future space exploration.

Beyond the Moon, samples from Mars and chondritic meteorites are also host to REEs, predominantly hosted in merrillite, in addition to apatite, whitlockite, xenotime, and recently-identified chevkinite-perrierite. These minor phases dominate the REE budget with abundances 1–2 orders of magnitude higher than their bulk host rock. However, as with the Moon, REEs have not yet been found in high enough concentrations in these extraterrestrial samples to warrant their classification as an ore resource. The concentrations of REEs in martian merrilites for example are several orders of magnitude lower than lunar merrillites, a difference attributed to the planetary bodies' crystallization history during the early evolution of the Solar System.

While the relative concentrations and abundances of the REEs in the phases that have been characterized to date provide crucial insights into the differentiation history of planetary objects, current and future missions to the Moon, Mars, and other nearby objects in our Solar System may yet reveal one or more extraterrestrial REE resources that one day will be utilized.

Acknowledgments: We thank Guest Editor Simon Jowitt for the opportunity to contribute to this special issue on the criticality of rare-earth elements. We are also very grateful to two anonymous reviewers who provided comments and thoroughly constructive feedback on an earlier draft of this manuscript. Our contribution was greatly improved by their input and suggestions.

Author Contributions: Claire L. McLeod designed the structure, collected the materials to be included in the review of REEs in planetary materials, and wrote 90% of this article. Mark P. S. Krekeler wrote the "The Criticality of REEs in Our Society" section discussing the current uses and demands for REEs, and claims a 10% authorship contribution.

Conflicts of Interest: The authors declare no conflict of interest.

References

1. Reinstein, E.R. Owning Outer Space. *Northwest. J. Int. Law Bus.* **1999**, *20*, 1.
2. Chakhmouradiani, A.R.; Wall, F. Rare Earth Elements: Minerals, Mines, Magnets (and More). *Elements* **2012**, *8*, 333–340. [CrossRef]
3. USGS. Rare Earths Statistics and Information. 2017. Available online: https://minerals.usgs.gov/minerals/pubs/commodity/rare_earths/ (accessed on 18 March 2017).
4. Haque, N.; Hughes, A.; Lim, S.; Vernon, C. Rare Earth Elements: Overview of Mining, Mineralogy, Uses, Sustainability and Environmental Impact. *Resources* **2014**, *3*, 614–635. [CrossRef]

5. Haskin, L.A.; Frey, F.A.; Schmitt, R.A.; Smith, R.H. Meteoritic, Solar and Terrestrial Rare-Earth Distributions. *Phys. Chem. Earth* **1966**, *7*, 167–321. [CrossRef]
6. Kynicky, J.; Smith, M.P.; Xu, C. Diversity of Rare Earth Deposits: The Key Example of China. *Elements* **2012**, *8*, 361–367. [CrossRef]
7. USGS. Mineral Commodities Survey, U.S. Department of the Interior. 2014. Available online: https://minerals.usgs.gov/minerals/pubs/mcs/2014/mcs2014.pdf (accessed on 31 March 2017).
8. Gray, T. *The Elements, a Visual Exploration of Every Known Atom in the Universe*; Black Dog and Leventhal Publishers: New York, NY, USA, 2012; 240p.
9. DOE. U.S. Department of Energy Critical Materials Strategy. 2011. Available online: https://energy.gov/sites/prod/files/DOE_CMS2011_FINAL_Full.pdf (accessed on 6 August 2017).
10. Golev, A.; Scott, M.; Erskine, P.D.; Ali, S.H.; Ballantyne, G.R. Rare earth supply chains: Current status, constraints and opportunities. *Resour. Policy* **2014**, *41*, 52–59. [CrossRef]
11. Goonan, T.G. *Rare Earth Elements—End Use and Recyclability*; Scientific Investigations Report 2011–5094; United States Geologic Survey. Available online: https://pubs.usgs.gov/sir/2011/5094/pdf/sir2011-5094.pdf (accessed on 6 August 2017).
12. Lewis, L.H.; Jimenez-Villacorta, F. Perspectives on permanent magnet materials for energy conversion and power generation. *Metall. Mater. Trans. A* **2013**, *44A*, 2–20. [CrossRef]
13. Graso, V.B. *Rare Earth Elements in National Defense: Background, Oversight Issues and Options for Congress*; Congressional Research Service Report 7-5700, R41744; Congressional Research Service, 2013; Available online: https://fas.org/sgp/crs/natsec/R41744.pdf (accessed on 21 May 2017).
14. Carrettin, S.; Concepcion, P.; Corma, A.; Nieto, J.M.L.; Puntes, V.F. Nanocrystalline CeO_2 increases the activity of Au for CO oxidation by two orders of magnitude. *Angew. Chem. Int. Ed.* **2004**, *43*, 2538–2540. [CrossRef] [PubMed]
15. Trovarelli, A.; de Leitenburg, C.; Boaro, M.; Dolcetti, G. The utilization of ceria in industrial catalysis. *Catal. Today* **1999**, *50*, 353–367. [CrossRef]
16. Gester, S.; Metz, P.; Zierau, O.; Vollmet, G. An efficient synthesis of the potent phytoestrogens 8-prenylnaringenin and 6-(1,1-dimethlyallyl)naringenin by europium(III)-catlyzed Claisen rearrangement. *Tetrahedron* **2001**, *57*, 1015–1018. [CrossRef]
17. Amin, S.; Voss, D.A.; Horrocks, W.D.; Lake, C.H.; Churchill, M.R.; Morrow, J.R. Laser-induced luminescence studies and crystal structure of the Europium(III) complex of 1,4,7,10-tetrakis(carbamoylmethyl)-1,4,7,10-tetraazacyclododecane—The link between phosphate diester binding and catalysis by lanthanide(III) macrocyclic complexes. *Inorg. Chem.* **1995**, *34*, 3294–3300. [CrossRef]
18. Gai, S.; Li, C.; Yang, P.; Lin, J. Recent progress in rare earth micro/nanocrystals: Soft chemical synthesis, luminescent properties, and biomedical applications. *Chem. Rev.* **2014**, *114*, 2343–2389. [CrossRef] [PubMed]
19. Gambogi, J. Rare Earths in Mineral Commodity summaries USGS. 2016. Available online: https://minerals.usgs.gov/minerals/pubs/commodity/rare_earths/mcs-2016-raree.pdf (accessed on 12 May 2017).
20. United Nations. *UNFPA Revision of Population Prospects*; United Nations, 2015; Available online: https://esa.un.org/unpd/wpp/publications/files/key_findings_wpp_2015.pdf (accessed on 8 May 2017).
21. Ali, S.H.; Giurco, D.; Arndt, N.; Nickless, E.; Borwn, G.; Demetriades, A.; Durrheim, R.; Enriquez, M.A.; Kinnaird, J.; Littleboy, A.; et al. Mineral supply for sustainable development requires resource governance. *Nature* **2017**, *543*, 367–372. [CrossRef] [PubMed]
22. Badescu, V. *Moon: Prospective Energy and Material Resources*; Springer: New York, NY, USA, 2012; 771p.
23. Crawford, I.A.; Joy, K.H. Lunar exploration: opening a window into the history and evolution of the inner Solar System. *Philos. Trans. R. Soc. A* **2014**, *372*, 20130315. [CrossRef] [PubMed]
24. Crawford, I.A. Lunar resources: A Review. *Prog. Phys. Geogr.* **2015**, *39*, 137–167. [CrossRef]
25. Crawford, I.A.; Anand, M.; Cockell, C.S.; Falcke, H.; Green, D.A.; Jaumann, R.; Wieczorek, M.A. Back to the Moon: The scientific rationale for resuming lunar surface exploration. *Planet. Space Sci.* **2012**, *74*, 3–14. [CrossRef]
26. Duke, M.B.; Gaddis, L.R.; Taylor, G.J.; Schmitt, H.H. Development of the Moon. In *New Views on the Moon*; Jolliff, B., Wieczorek, M., Shearer, C., Neal, C., Eds.; Mineralogical Society of America: Chantilly, VA, USA, 2006; Volume 60.

27. Aldridge, E.C.; Fiorina, C.S.; Jackson, M.P.; Leshin, L.A.; Lyles, L.L.; Spudis, P.D.; Tyson, N.D.; Walker, R.S.; Zuber, M.T. *A Journey to Inspire, Innovate and Discover, Report of the President's Commission on Implementation of United States Space Exploration Policy*; U.S. Government Printing Office: Washington, DC, USA, 2004.
28. Carpenter, J.; Fisackerly, R.; Houdou, B. Establishing lunar resource viability. *Space Policy* **2016**, *37*, 52–57. [CrossRef]
29. Chamberlain, P.G.; Taylor, L.A.; Podnieks, E.R.; Miller, R.J. A review of possible mining applications in space. In *Resources of Near-Earth Space*; Lewis, J.S., Matthews, M.S., Guerrieri, M.L., Eds.; University of Arizona Press: Tucson, AZ, USA, 1992; pp. 51–68.
30. Shishko, R.; Fradet, R.; Saydam, S.; Tapia-Cortez, C.; Dempster, A.; Coulton, J.; Do, S. An Integrated Economics Model for ISRU in Support of a Mars Colony—Initial Results Report. In Proceedings of the 10th Symposium on Space Resource Utilization, AIAA SciTech Forum (AIAA 2017-0422), Grapevine, TX, USA; 2015. Available online: https://arc.aiaa.org/doi/pdf/10.2514/6.2017-0422 (accessed on 6 August 2017).
31. Wang, K.-T.; Lemouhna, P.N.; Tang, Q.; Li, W.; Cui, X.-M. Lunar regolith can allow the synthesis of cement materials with near-zero water consumption. *Gondwana Res.* **2017**, *44*, 1–6. [CrossRef]
32. ASI; BNSC; CNES; CNSA; CSA; CSIRO; DLR; ESA; ISRO; JAXA; KARL; NASA; NSAU; Roscosmos. The Global Exploration Strategy: The Framework for Coordination, 2007. Available online: https://www.nasa.gov/pdf/296751main_GES_framework.pdf (accessed on 1 May 2017).
33. Wood, J.A.; Dickey, J.S.; Marvin, U.B.; Powell, B.M. Lunar anorthosites and a geophysical model of the Moon. In Proceedings of the Apollo 11 Lunar Science Conference, Houston, TX, USA, 5–8 January 1970; Pergamon: New York, NY, USA, 1970; pp. 965–988.
34. Smith, J.V.; Andersen, A.T.; Newton, R.C.; Olsen, E.J.; Crewe, A.V.; Isaacson, M.S.; Johnson, D.; Wyllie, P.J. Petrologic history of the Moon inferred from petrography, mineralogy, and petrogenesis of the Apollo 11 rocks. In Proceedings of the Apollo 11 Lunar Science Conference, Houston, TX, USA, 5–8 January 1970; Pergamon Press: New York, NY, USA, 1970; pp. 897–926.
35. Taylor, S.R.; Jakes, P. The geochemical evolution of the moon. Proceedings of 5th Lunar Science Conference, Houston, TX, USA, 18–22 March 1974; pp. 1287–1305.
36. Taylor, S.R. *Lunar Science: A Post-Apollo View*; Pergamon Press: New York, NY, USA, 1975; p. 372.
37. Taylor, S.R. Structure and evolution of the moon. *Nature* **1979**, *281*, 105–110. [CrossRef]
38. Shirley, D.N. A partially molten magma ocean model. *J. Geophys. Res.* **1983**, *88*, A519–A527. [CrossRef]
39. Warren, P.W. The lunar magma ocean concept and lunar evolution. *Ann. Rev. Earth Planet. Sci.* **1985**, *13*, 201–240. [CrossRef]
40. Heiken, G.H.; Vaniman, D.T.; French, B.M. (Eds.) *Lunar Sourebook a User's Guide to the Moon*; Cambridge University Press and the Lunar Planetary Institute: Cambridge, UK, 1991; 736p.
41. Snyder, G.A.; Taylor, L.A.; Neal, C.R. A chemical model for generating the sources of mare basalts: combined equilibrium and fractional crystallization of the lunar magmasphere. *Geochim. Cosmochim. Acta* **1992**, *56*, 3809–3823. [CrossRef]
42. Papike, J.J.; Ryder, G.; Shearer, C.K. Lunar Materials. In *Planetary Materials, Reviews in Mineralogy*; Papike, J.J., Ed.; Mineralogical Society of America: Washington, DC, USA, 1998; Volume 36, pp. 5.1–5.23.
43. Jolliff, B.L.; Wieczorek, M.A.; Shearer, C.K.; Neal, C.R. (Eds.) *New Views of the Moon*; Reviews in Mineralogy and Geochemistry, Mineralogical Society of America: Chantilly, VA, USA, 2006; Volume 60, p. 721.
44. Longhi, J. Petrogenesis of the picritic mare magmas: on constraints on the extent of early lunar differentiation. *Geochim. Cosmochim. Acta* **2006**, *70*, 5919–5934. [CrossRef]
45. Touboul, M.; Kleine, T.; Bourdon, B.; Palme, H.; Wieler, R. Late formation and prolonged differentiation of the Moon inferred from W isotopes in lunar metals. *Nature* **2007**, *450*, 1206–1209. [CrossRef] [PubMed]
46. Halliday, A.N. A young Moon-forming giant impact 70–110 million years ago accompanied by late-stage mixing, core formation and degassing of the Earth. *Philos. Trans. R. Soc.* **2008**, *366*, 4163–4181. [CrossRef] [PubMed]
47. Brandon, A.D.; Lapen, T.J.; Debaille, V.; Beard, B.K.; Rankenburg, K.; Neal, C. Re-evaluating $^{142}Nd/^{144}Nd$ in lunar mare basalts with the implications for the early evolution and bulk Sm/Nd of the Moon. *Geochim. Cosmochim. Acta* **2009**, *73*, 6421–6445. [CrossRef]
48. Kleine, T.; Touboul, M.; Bourdon, B.; Nimmo, F.; Mezger, K.; Palme, H.; Jacobsen, S.B.; Yin, Q.-Z.; Halliday, A.N. Hf-W chronology of the accretion and early evolution of asteroids and terrestrial planets. *Geochim. Cosmochim. Acta* **2009**, *73*, 5150–5188. [CrossRef]

49. Borg, L.E.; Connelly, J.N.; Boyet, M.; Carlson, R.W. Chronological evidence that the Moon is either young or did not have a global magma ocean. *Science* **2011**, *477*, 70–72. [CrossRef] [PubMed]
50. Elardo, S.M.; Draper, D.S.; Shearer, C.K. Lunar magma ocean crystallization revisited: bulk composition, early cumulate mineralogy and the source regions of the Mg-suite. *Geochim. Cosmochim. Acta* **2011**, *75*, 3024–3045. [CrossRef]
51. Elkins-Tanton, L.T. Magma oceans in the inner solar system. *Ann. Rev. Earth Planet. Sci.* **2012**, *40*, 113–139. [CrossRef]
52. Jacobson, S.A.; Mobirdelli, A.; Rayond, S.N.; O'Brien, D.P.; Walsh, K.J.; Rubie, D.C. Highly siderophile elements in Earth's mantle as a clock for the Moon-forming impact. *Nature* **2014**, *508*, 84–87. [CrossRef] [PubMed]
53. McLeod, C.L.; Brandon, A.D.; Armytage, R.M.G. Constraints on the formation age and evolution of the Moon from ^{142}Nd-^{143}Nd systematics of Apollo 12 basalts. *Earth Planet. Sci. Lett.* **2014**, *396*, 179–189. [CrossRef]
54. McLeod, C.L.; Brandon, A.D.; Fernandes, V.A.; Peslier, A.H.; Fritz, J.; Lapen, T.; Shafer, J.T.; Butcher, A.R.; Irving, A.J. Constraints on formation and evolution of the lunar crust from feldspathic granultic breccias NWA 3163 and 4881. *Geochim. Cosmochim. Acta* **2016**, *187*, 350–374. [CrossRef]
55. Borg, L.E.; Gaffney, A.M.; Shearer, C.K. A review of lunar chronology revealing a preponderance of 4.34–4.37 Ga ages. *Meteorit. Planet. Sci.* **2015**, *50*, 715–732. [CrossRef]
56. Boyce, J.W.; Treiman, A.H.; Guan, Y.; Ma, C.; Eiler, J.M.; Gross, J.; Greenwood, J.P.; Stolper, E.M. The chlorine isotope fingerprint of the lunar magma ocean. *Sci. Adv.* **2015**, *1*, 1–8. [CrossRef] [PubMed]
57. Barr, A.C. On the origin of the Earth's Moon. *J. Geophys. Res. Planets* **2016**, *121*, 1573–1601. [CrossRef]
58. Sivakumar, V.; Neekakantan, R.; Santosh, M. Lunar surface mineralogy using hyperspectral data: Implications for primordial crust in the Earth-Moon system. *Geosci. Front.* **2017**, *8*, 457–465. [CrossRef]
59. Sun, C.; Graff, M.; Liang, Y. Trace element partitioning between plagioclase and silicate melt: The importance of temperature and plagioclase composition, with implications for terrestrial and lunar magnetism. *Geochim. Cosmochim. Acta* **2017**, *206*, 273–295. [CrossRef]
60. Google LUNAR XPRIZE, 2017. Available online: http://lunar.xprize.org/ (accessed on 4 June 2017).
61. Moon Express. 2016. Available online: http://www.moonexpress.com/files/moon-express-press-kit.pdf (accessed on 4 June 2017).
62. Caminiti, S. The Billionaire's Race to Harness the Moon's Resources. Available online: http://www.cnbc.com/2014/04/02/the-global-race-to-harness-the-Moon\T1\textquoterights-resources.html (accessed on 5 August 2017).
63. Goins, N.R.; Dainty, A.M.; Toksoz, M.N. Lunar seismology: The internal structure of the Moon. *J. Geophys. Res.* **1981**, *86*, 5061–5074. [CrossRef]
64. Wieczorek, M.A.; Jolliff, B.L.; Khan, A.; Pritchard, M.E.; Weiss, B.P.; Williams, J.G.; Hood, L.L.; Righter, K.; Neal, C.R.; Shearer, C.K.; et al. The Constitution and Structure of the Lunar Interior. *Rev. Mineral. Geochem.* **2006**, *60*, 221–364. [CrossRef]
65. Weber, R.C.; Lin, P.-Y.; Garnero, E.J.; Williams, Q.; Lognonne, P. Seismic Detection of the Lunar Core. *Science* **2011**, *331*, 309–312. [CrossRef] [PubMed]
66. Jaumann, R.; Hiesinger, H.; Anand, M.; Crawford, I.A.; Wagner, R.; Sohl, F.; Jolliff, B.L.; Scholten, F.; Knapmeyer, M.; Hoffman, H.; et al. Geology, geochemistry and geophysics of the Moon: Status of current understanding. *Planet. Space Sci.* **2012**, *74*, 15–41. [CrossRef]
67. Haskin, L.A.; Colson, R.O.; Vaniman, D.T.; Gillett, S.L. A geochemical assessment of possible lunar ore formation. In *Resources of Near-Earth Space*; Lewis, J.S., Matthews, M.S., Guerrieri, M.L, Eds.; University of Arizona Press: Tucson, AZ, USA, 1993; 977p.
68. Solomon, S.C.; Toksoz, M.N. Internal Constitution and Evolution of the Moon. *Phys. Earth Planet. Inter.* **1973**, *7*, 15–38. [CrossRef]
69. Elkins-Tanton, L.T.; Burgess, S.; Yin, Q.-Z. The lunar magma ocean: Reconciling the solidification process with lunar petrology and geochronology. *Earth Planet. Sci. Lett.* **2011**, *304*, 326–336. [CrossRef]
70. McLeod, C.L. Lunar Magma Ocean, Size. In *Encyclopedia of Lunar Science*; Cudnik, B., Ed.; Springer: New York, NY, USA, 2016. [CrossRef]
71. Wieczorek, M.A.; Neumann, G.A.; Nimmo, F.; Kiefer, W.S.; Taylor, G.J.; Melosh, H.J.; Phillips, R.J.; Solomon, S.C.; Andrews-Hanna, J.C.; Asmar, S.W.; et al. The Crust of the Moon as Seen by GRAIL. *Science* **2013**, *339*, 671–675. [CrossRef] [PubMed]

72. Petro, N.E.; Jolliff, B.L. Thin Crust in the South Pole Aitken Basin and Samples from the Mantle? Implications for the South Pole-Aitken Basin Sampling in light of Recent GRAIL Results. In Proceedings of the 44th Lunar Planetary Science Conference, Woodlands, TX, USA, 18–22 March 2013; p. 2724.
73. Green, D.H.; Ringwood, A.E. The stability fields of aluminous pyroxene peridotite and garnet peridotite. *Earth Planet. Sci. Lett.* **1967**, *3*, 151–160. [CrossRef]
74. Longhi, J. A model of early lunar differentiation. In Proceedings of the 11st Lunar and Planetary Science Conference, Houston, TX, USA, 17–21 March 1980; pp. 289–315.
75. Shearer, C.K.; Papike, J.J. Magmatic evolution of the Moon. *Am. Mineral.* **1999**, *84*, 1469–1494. [CrossRef]
76. Hiesinger, H.; Jaumann, R.; Neukum, G.; Head, J.W., III. Ages of mare basalts on the lunar nearside. *J. Geophys. Res.* **2000**, *105*, 29239–29275. [CrossRef]
77. Braden, S.E.; Stopar, J.S.; Robinson, M.S.; Lawrence, S.J.; van der Bogert, C.H.; Hiesenger, H. Evidence for basaltic volcanism on the Moon within the past 100 million years. *Nat. Geosci.* **2014**, *7*, 787–791. [CrossRef]
78. Green, D.H.; Ringwood, A.E.; Ware, N.G.; Hibberson, A.; Kiss, E. Experimental petrology and petrogenesis of Apollo 12 basalts. In Proceedings of the 2nd Lunar Science Conference, Houston, TX, USA, 11–14 January 1971; pp. 601–615.
79. Green, D.H.; Ware, N.G.; Hibberson, A.; Major, A. Experimental petrology of Apollo 12 mare basalts, Part 1, sample 12009. *Earth Planet. Sci. Lett.* **1971**, *13*, 85–96. [CrossRef]
80. Philpotts, J.A.; Schnetzler, C.C.; Nava, D.D.; Bottino, M.L.; Fullagar, P.D.; Thomas, H.H.; Schumann, S.; Kouns, C.W. Apollo 14: some geochemical aspects. Proceedings of Third Lunar Planetary Science Conference, Houston, TX, USA, 10–13 January 1972; The MIT Press; pp. 1293–1305. Available online: http://adsabs.harvard.edu/full/1972LPSC....3.1293P (accessed on 28 May 2017).
81. Haskin, L.A.; Lindstrom, M.M.; Salpas, P.A.; Lindstrom, D. On compositional variations among lunar anorthosites. In Proceedings of the 12th Lunar Science Conference, Houston, TX, USA, 16–20 March 1981; pp. 41–66.
82. Morse, S.A. Adcumulus growth of anorthosite at the base of the lunar crust. In Proceedings of the 13th Lunar and Planetary Science Conference, Houston, TX, USA, 15–19 March 1982; pp. A10–A18.
83. Ryder, G. Lunar anorthosite 60025, the petrogenesis of lunar anorthosites, and the bulk composition of the Moon. *Geochem. Cosmochim. Acta* **1982**, *46*, 1591–1601. [CrossRef]
84. Longhi, J. Origin of Picritic Green Glass Magmas by Polybaric Fractional Fusion. *Proc. Lunar Planet. Sci.* **1992**, *22*, 343–353.
85. Warren, P.W.; Wasson, J.T. Compositional-petrographic investigation of pristine nonmare rocks. In Proceedings of the 9th Lunar and Planetary Science Conference, Houston, TX, USA, 13–17 March 1978; pp. 185–217.
86. Yanhao, L.; Tronche, E.J.; Steenstra, E.S.; van Westrenen, W. Experimental constraints on the solidification of a nominally dry lunar magma ocean. *Earth Planet. Sci. Lett.* **2017**, *471*, 104–116.
87. Alibert, C.; Norman, M.D.; McCulloch, M.T. An ancient Sm-Nd age for a ferroan noritic anorthosite clast from lunar breccia 67016. *Geochim. Cosmochim. Acta* **1994**, *58*, 2921–2926. [CrossRef]
88. Borg, L.E.; Gaffney, A.M.; Shearer, C.K.; DePaolo, D.J.; Hutcheon, I.D.; Owens, T.L.; Ramon, E.; Brennecka, G. Mechanisms for incompatible-element enrichment on the Moon deduced from the lunar basaltic meteorite Northwest Africa 032. *Geochim. Cosmochim. Acta* **2009**, *73*, 3963–3980. [CrossRef]
89. Meyer, J.; Elkins Tanton, L.T.; Wisdom, J. Coupled thermal-orbital evolution of the early Moon. *Icarus* **2010**, *208*, 1–10. [CrossRef]
90. Taylor, D.J.; McKeegan, K.D.; Harrison, T.M. Lu-Hf zircon evidence for rapid lunar differentiation. *Earth Planet. Sci. Lett.* **2009**, *279*, 157–264. [CrossRef]
91. Gaffney, A.M.; Borg, L.E. A Young Age for KREEP Formation Determined from Lu-Hf Isotope Systematics of KREEP Basalts and Mg-Suite Samples. In Proceedings of the 44th Lunar and Planetary Science Conference, Woodlands, TX, USA, 18–22 March 2013; p. 1719.
92. Smith, J.V.; Steele, I.M. Lunar mineralogy: A heavenly detective story. Part II. *Am. Mineral.* **1976**, *61*, 1059–1116.
93. Meyer, C. NASA Lunar Petrographic Educational Thin Section Set. 2003. Available online: https://curator.jsc.nasa.gov/lunar/letss/mineralogy.pdf (accessed on 18 March 2017).
94. Meyer, C. *Lunar Sample Compendium*; Lunar Planetary Institute: Houston, TX, USA, 2009.
95. Frondel, J.W. *Lunar Mineralogy*; Wiley-Interscience: New York, NY, USA, 1975; pp. 84–87.

96. Yazawa, Y.; Yamaguchi, A.; Takeda, H. Lunar Minerals and Their Resource Utilization with Particular Reference to Solar Power Satellite and Potential Roles for Humic substances for Lunar Agriculture. In *Moon, Prospective Energy and Material Resources*; Badescu, V., Ed.; Springer: New York, NY, USA, 2012; 771p.
97. Dixon, J.R.; Papike, J.J. Petrology of anorthosites from the Descartes region of the moon: Apollo 16. In Proceedings of the 6th Lunar Science Conference, Houston, TX, USA, 17–21 March 1975; pp. 263–291.
98. James, O.B.; Lindstrom, M.M.; McGee, J.J. Lunar ferroan anorthosite 60025: Petrology and chemistry of mafic lithologies. In Proceedings of the 21st Lunar Planetary Science Conference, Houston, TX, USA, 12–16 March 1990; Lunar Planetary Institute: Houston, TX, USA.
99. Brown, G.M.; Emeleus, C.H.; Holland, G.J.; Peckett, A.; Phillips, R. Mineral-chemical variations in Apollo 14 and Apollo 15 basalts and granitic fractions. In Proceedings of the 3rd Lunar Science Conference, Houston, TX, USA, 10–13 January 1972; pp. 147–157.
100. Papike, J.J.; Hodges, F.N.; Bence, A.E.; Cameron, M.; Rhodes, J.M. Mare basalts: Crystal chemistry, mineralogy and petrology. *Rev. Geophys. Space Phys.* **1976**, *14*, 475–540. [CrossRef]
101. McGee, P.E.; Warner, J.L.; Simonds, C.H. *Introduction to the Apollo Collections. Part I: Lunar Igneous Rocks*; Curators Office, JSC, 1977; Available online: http://www.lpi.usra.edu/lunar/surface/apolloCollectionsPartI.pdf (accessed on 28 May 2017).
102. Lunar Sample Atlas. Available online: http://www.lpi.usra.edu/lunar/samples/atlas/thin_sections/ (accessed on 12 March 2017).
103. Warren, P.H.; Wasson, J.T. The Origin of KREEP. *Rev. Geophys. Space Phys.* **1979**, *17*, 73–88. [CrossRef]
104. Shearer, C.K.; Hess, P.C.; Wieczorek, M.A.; Prichard, M.E.; Parmentier, E.M.; Borg, L.E.; Longhi, J.; Elkins-Tanton, L.T.; Neal, C.R.; Antonenko, I.; et al. Thermal and Magmatic Evolution of the Moon. *Rev. Mineral. Geochem.* **2006**, *60*, 365–518. [CrossRef]
105. Lawrence, D.J.; Feldman, W.C.; Barraclough, B.L.; Elphic, R.C.; Maurice, S.; Binder, A.B.; Miller, M.C.; Prettyman, T.H. High resolution measurements of absolute thorium abundances on the lunar surface from the Lunar Prospector gamma-ray spectrometer. *Geophys. Res. Lett.* **1999**, *26*, 2681–2684. [CrossRef]
106. Haskin, L.A.; Gillis, J.J.; Korotev, R.L.; Jolliff, B.L. The Materials of the lunar Procellarum KREEP Terrane: A synthesis of data from geomorphological mapping, remote-sensing, and sample analysis. *J. Geophys. Res.* **2000**, *105*, 20403–20415. [CrossRef]
107. Jolliff, B.L.; Gillis, J.J.; Haskin, L.A.; Korotev, R.L.; Wieczorek, M.A. Major lunar crustal terranes: Surface expressions and crust-mantle origins. *J. Geophys. Res. Planets* **2000**, *105*, 4197–4216. [CrossRef]
108. Global Map of the Element Thorium. Available online: https://solarsystem.nasa.gov/galleries/global-map-of-the-element-thorium (accessed 21 August 2017).
109. Wieczorek, M.A.; Phillips, R.J. Lunar multi-ring basins and the cratering process. *Icarus* **1999**, *139*, 246–259. [CrossRef]
110. Lawrence, D.J.; Feldman, W.C.; Barraclough, B.L.; Binder, A.B.; Elphic, R.C.; Maurice, S.; Miller, M.C.; Prettyman, T.H. Thorium abundances on the lunar surface. *J. Geophys. Res.* **2000**, *105*, 20307–20331. [CrossRef]
111. Zou, Y.; Xu, L.; Ouyang, Z. KREEP Rocks. *Chin. J. Geochem.* **2004**, *23*, 65–70.
112. Neal, C.L.; Taylor, L.A. *Definition of a Pristine, Unadulterated urKREEP Composition Using the "K-FRAC/REEP-FRAC" Hypothesis*. Abstracts of the Lunar and Planetary Science Conference. 1989, Volume 20, pp. 772–773. Available online: http://adsabs.harvard.edu/full/1989LPI....20..772N (accessed on 27 May 2017).
113. Neal, C.L.; Taylor, L.A. Metasomatic products of the lunar magma ocean: The role of KREEP dissemination. *Geochim. Cosmochim. Acta* **1989**, *53*, 529–541. [CrossRef]
114. Thompson, R.N. British Tertiary volcanic province. *Scott. J. Geol.* **1982**, *18*, 49–107. [CrossRef]
115. Lindstrom, M.M.; Knapp, S.A.; Shervais, J.A.; Taylor, L.A. Magnesian anorthosites and associated troctolites and dunite in Apollo 14 breccias. In Proceedings of the 15th Lunar and Planetary Science Conference, Houston, TX, USA, 12–16 March 1984; pp. C41–C49.
116. Rudnick, R.L.; Gao, S. Composition of the Continental Crust. *Treatise Geochem.* **2003**, *3*, 1–64.
117. Warren, P.H.; Jerde, E.A.; Kalleymeyn, G.W. Pristine moon rocks: A "large" felsite and metal-rich ferroan anorthosite. In Proceedings of the 17th Lunar and Planetary Science Conference, Houston, TX, USA.

118. Jolliff, B.L.; Wadhwa, M. The distribution of Rare Earth Elements between Lunar apatite and whitlockite. In Proceedings of the 23rd Lunar and Planetary Science Conference, Houston, TX, USA, 16–20 March 1992; pp. 625–626.
119. Kartashov, P.M.; Bogatikov, O.A.; Mokhov, A.V.; Gorshkov, A.I.; Ashikhmina, N.A.; Magazina, L.O.; Koporulina, E.V. Lunar Monazites. In *Doklady Earth Sciences*; MAIK Nauka/Interperiodica, 2006; Volume 407A, pp. 498–502. Available online: https://link.springer.com/article/10.1134/S1028334X06030342 (accessed on 21 August 2017).
120. Jolliff, B.L.; Hughes, J.M.; Freeman, J.J.; Ziegler, R.A. Crystal chemistry of lunar merrillite and comparison to other meteoritic and planetary suites of whitlockite and merrillite. *Am. Mineral.* **2006**, *91*, 1583–1595. [CrossRef]
121. Jolliff, B.L. Fragments of Quartz Monzodiorite and Felsite in Apollo 14 Soil Particles. In Proceedings of the Lunar and Planetary Science Conference, Houston, TX, USA, 12–16 March 1990; Volume 21, pp. 101–118.
122. Jolliff, B.L. Large-Scale Separation of K-frac and REEP-frac in the source Regions of Apollo Impact-Melt Breccias, and a Revised Estimate of the KREEP Composition. *Int. Geol. Rev.* **1998**, *40*, 916–935. [CrossRef]
123. Meyer, C.; Yang, S.V. Tungsten-bearing yttrobetafite in lunar granophyre. *Am. Mineral.* **1988**, *73*, 1420–1425.
124. Ramdohr, P.; El Gorsey, A. Opaque minerals of the lunar rocks and dust from Mare Tranquillitatis. *Science* **1970**, *167*, 615–618. [CrossRef] [PubMed]
125. Cameron, E.N. Opaque minerals in certain lunar rocks from Apollo 11. In Proceedings of the Apollo 11 Lunar Science Conference, Houston, TX, USA, 5–8 January 1970; pp. 221–245.
126. Lovering, J.F.; Wark, D.A.; Reid, A.F.; Ware, N.G.; Keil, K.; Prinz, M.; Bunch, T.E.; El Gorsey, A.; Ramdohr, P.; Brown, G.M.; et al. Tranquillityite: A new silicate mineral from Apollo 11 and Apollo 12 basaltic rocks. In Proceedings of the Lunar Science Conference, Houston, TX, USA, 11–14 January 1971; Volume 2, pp. 39–45.
127. Rasmussen, B.; Fletcher, I.R.; Gregory, C.J.; Muhling, J.R.; Suvorova, A.A. Tranquillityite: The last lunar mineral comes down to Earth. *Geology* **2012**, *40*, 83–86. [CrossRef]
128. Haskin, L.A.; Warren, P. Lunar Chemistry. In *The Lunar Sourcebook: A User's Guide to the Moon*; Cambridge University Press: Cambridge, UK, 1991; pp. 357–474.
129. McKay, D.S.; Heiken, G.; Basu, A.; Blanford, G.; Simon, S.; Reedy, R.; French, B.M.; Papike, J. The lunar regolith. In *Lunar Sourcebook*; Heiken, G.H., Vaniman, D.T., French, B.M., Eds.; Cambridge University Press: Cambridge, UK, 1991; pp. 285–356.
130. Blair, B. Quantitative Approaches to Lunar Economic Analysis. In Proceedings of the Annual Meeting of the Lunar Exploration Analysis Group (LEAG), Houston, TX, USA; 2009. Available online: http://www.lpi.usra.edu/meetings/leag2009/presentations/Day-1%20PM/02-15_Blair.pdf (accessed on 6 August 2017).
131. Santiago-Maldonado, E.; Gleaton, J.; Devor, R.; Captain, J. Creating Methane from Plastic: Recycling at a Lunar Outpost. In Proceedings of the 48th AIAA Aerospace Sciences Meeting including the New Horizons Forum and Aerospace Exposition, Orlando, FL, USA, 4–7 January 2010; American Institute of Aeronautics and Astronautics: Reston, VA, USA, 2010; Volume 21, pp. 18271–18278.
132. Hintze, P.E.; Quintana, S. Building a Lunar or Martian Launch Pad with In Situ Materials: Recent Laboratory and Field Studies. *J. Aerosp. Eng.* **2013**, *26*, 134–142. [CrossRef]
133. Schrunk, D.; Sharp, B.; Cooper, B.; Thangavelu, M. *The Moon: Resources, Future Development, and Settlement*; Springer: Chichester, UK, 2008.
134. Anand, M.; Crawford, I.A.; Balat-Pichelin, M.; Abanades, S.; van Westrenen, W.; Péraudeau, G.; Jaumann, R.; Seboldt, W. A brief review of chemical and mineralogical resources on the Moon and likely in situ resource utilization (ISRU) applications. *Planet. Space Sci.* **2012**, *74*, 42–48. [CrossRef]
135. Fegley, B.; Swindle, T.D. Lunar volatiles: Implications for lunar resource utilization. In *Resources of Near Earth Space*; Lewis, J., Matthews, M.S., Guerrieri, M.L., Eds.; Tucson University Press: Tucson, AZ, USA, 1993; pp. 367–426.
136. Fa, W.; Jin, Y.-Q. Quantitative estimation of helium-3 spatial distribution in the lunar regolith layer. *Icarus* **2007**, *190*, 15–23. [CrossRef]
137. Feldman, W.C.; Maurice, S.; Binder, A.B.; Barraclough, B.L.; Elphic, R.C.; Lawrence, D.J. Fluxes of fast and epithermal neutrons from Lunar Prospector: Evidence for water ice at the lunar poles. *Science* **1998**, *281*, 1496–1500. [CrossRef] [PubMed]

138. Feldman, W.C.; Maurice, S.; Lawrence, D.J.; Little, R.C.; Lawson, S.L.; Gasnault, O.; Wiens, R.C.; Barraclough, B.L.; Elphic, R.C.; Prettyman, T.H.; et al. Evidence for water ice near the lunar poles. *J. Geophys. Res.* **2011**, *106*, 23231–23252. [CrossRef]
139. Colaprete, A.; Schultz, P.; Heldmann, J.; Wooden, D.; Shirley, M.; Ennico, K.; Hermalyn, B.; Marshall, W.; Ricco, A.; Elphic, R.C.; et al. Detection of Water in the LCROSS Ejecta Plume. *Science* **2010**, *330*, 463–468. [CrossRef] [PubMed]
140. USGS. 2016. Available online: https://water.usgs.gov/edu/qa-home-percapita.html (accessed on 19 March 2017).
141. Taylor, L.A.; Carrier, W.D. Oxygen production on the Moon: An overview and evaluation. In *Resources of Near Earth Space*; Lewis, J., Matthews, M.S., Guerrieri, M.L., Eds.; Tucson University: Tucson, AZ, USA, 1993.
142. Schwandt, C.; Dimitrov, A.T.; Fray, D.J. High-yield synthesis of multi-walled carbon nanotubes from graphite by molten salt electrolysis. *Carbon* **2012**, *50*, 1311–1315. [CrossRef]
143. Benaroya, H.; Mottaghi, S.; Porter, Z. Magnesium as an ISRU-derived resource for lunar structures. *J. Aerosp. Eng.* **2013**, *26*, 152–159. [CrossRef]
144. Mottaghi, S.; Benaroya, H. Design of a Lunar Surface Structure. I: Design Configuration and Thermal Analysis. *J. Aerosp. Eng.* **2015**, *28*, 0401405. [CrossRef]
145. NASA. Metals from Regolith. 2012. Available online: https://isru.nasa.gov/MetalsfromRegolith.html (accessed on 7 August 2017).
146. Lucey, P.G.; Taylor, G.J.; Malaret, E. Abundance and distribution of iron on the Moon. *Science* **1995**, *268*, 1150–1153. [CrossRef] [PubMed]
147. Meyers, C.; Toutanji, H. Analysis of Lunar-Habitat Structure Using Waterless Concrete and Tension glass Fibers. *J. Aerosp. Eng.* **2007**, *20*, 220–226. [CrossRef]
148. Masafumi, I.; Gertsch, L. Excavation of Lunar Regolith with Large Grains by Rippers for Improved Excavation Efficiency. *J. Aerosp. Eng.* **2013**, *26*, 97–104.
149. Wilhelm, S.; Curbach, M. Review of possible mineral materials and production techniques for a building material on the moon. *Struct. Concr.* **2014**, *15*, 419–428. [CrossRef]
150. Turkevich, A. Average chemical composition of the lunar surface. In Proceedings of the 4th Lunar Science Conference, Houston, TX, USA, 5–8 March 1973; Volume 2, pp. 1119–1168.
151. Papike, J.J.; Simon, S.B.; Laul, J.C. Lunar Regolith: Chemistry, Mineralogy, and Petrology. *Rev. Geophys.* **1982**, *20*, 761–826. [CrossRef]
152. Lucey, P.G.; Korotev, R.L.; Gillis, J.J.; Taylor, L.A.; Lawrence, D.; Campbell, B.A.; Elphic, R.; Feldman, B.; Hood, L.L.; Hunten, D.; et al. Understanding the lunar surface and space-Moon interaction. *Rev. Mineral. Geochem.* **2006**, *60*, 82–219. [CrossRef]
153. Ceccanti, F.; Dini, E.; De Kestelier, X.; Colla, V.; Pambaguian, L. 3D printing technology for a moon outpost exploiting lunar soil. In Proceedings of the 61st International Astronautical Congress, Prague, Czech Republic, 27 September–1 October 2010; Available online: http://esmat.esa.int/Publications/Published_papers/IAC-10-D3.3.5.pdf (accessed on 23 August 2017).
154. Cesaretti, G.; Dini, E.; De Kestelier, X.; Colla, V.; Pambaguian, L. Building components for an outpost on the Lunar soil by means of a novel 3D printing technology. *Acta Astron.* **2014**, *93*, 430–450. [CrossRef]
155. Norman, M.D. The composition and thickness of the crust of Mars estimated from rare earth elements and neodymium-isotopic compositions of Martian meteorites. *Meteorit. Planet. Sci.* **1999**, *34*, 439–449. [CrossRef]
156. An up-to-date List of Martian Meteorites. Available online: http://www.imca.cc/mars/martian-meteorites-list.htm (accessed on 21 August 2017).
157. List of Lunar Meteorites. Available online: http://meteorites.wustl.edu/lunar/moon_meteorites_list_alpha.htm (accessed on 21 August 2017).
158. Apollo Missions. Available online: http://www.lpi.usra.edu/lunar/missions/apollo/ (accessed on 21 August 2017).
159. Taylor, G.J. A Primordial and Complicated Ocean of Magma on Mars. Planetary Science Research Discoveries, 2006. Available online: http://www.psrd.hawaii.edu/Mar06/mars_magmaOcean.html (accessed on 7 August 2017).
160. Harper, C.L.; Nyquist, L.E.; Bansal, B.; Wiesmann, H.; Shih, C.-Y. Rapid accretion and early differentiation of Mars as indicated by $^{142}Nd/^{144}Nd$ in SNC meteorites. *Science* **1995**, *267*, 213–216. [CrossRef] [PubMed]

161. Borg, L.E.; Nyquist, L.E.; Taylor, L.A.; Wiesmann, H.; Shih, C.-Y. Constraints on Martian differentiation processes from Rb-Sr and Sm-Nd isotopic analyses of the basaltic shergottite QUE 94201. *Geochim. Cosmochim. Acta* **1997**, *61*, 4915–4931. [CrossRef]
162. Lee, D-C.; Halliday, A.N. Core formation on Mars and differentiated asteroids. *Nature* **1997**, *388*, 854–857. [CrossRef]
163. Halliday, A.N.; Wänke, H.; Birck, J.-L.; Clayton, R.N. The Accretion, Composition and Early Differentiation of Mars. *Space Sci. Rev.* **2001**, *96*, 197–230. [CrossRef]
164. Elkins-Tanton, L.T.; Parmentier, E.M.; Hess, P.C. Magma ocean fractional crystallization and cumulate overturn in terrestrial planets: Implications for Mars. *Meteorit. Planet. Sci.* **2003**, *38*, 1753–1771. [CrossRef]
165. Elkins-Tanton, L.T.; Hess, P.C.; Parmentier, E.M. Possible formation of ancient crust on Mars through magma ocean processes. *J. Geophys. Res.* **2005**, *110*, E12S01. [CrossRef]
166. Foley, C.N.; Wadhwa, M.; Borg, L.E.; Janney, P.E.; Hines, R.; Grove, T.L. The early differentiation history of Mars from ^{182}W-^{142}Nd isotope systematics in the SNC meteorites. *Geochim. Cosmochim. Acta* **2005**, *69*, 4557–4571. [CrossRef]
167. Solomon, S.C.; Aharonson, O.; Aurnou, J.M.; Banerdt, B.W.; Carr, M.H.; Dombard, A.J.; Frey, H.V.; Golombek, M.P.; Hauck, S.A., II; Head, J.W., III; et al. New Perspectives on American Mars. *Science* **2005**, *307*, 1214–1220. [CrossRef] [PubMed]
168. Borg, L.E.; Draper, D.S. A petrogenetic model for the origin and compositional variation of the Martian basaltic meteorites. *Meteorit. Planet. Sci.* **2003**, *38*, 1713–1731. [CrossRef]
169. Boynton, W.V.; Taylor, G.J.; Evans, L.G.; Reedy, R.C.; Starr, R.; Janes, D.M.; Kerry, K.E.; Drake, D.M.; Kim, K.J.; Williams, R.M.S.; et al. Concentration of H, Si, Cl, K, Fe, and Th in the low- and mid-latitude regions of Mars. *J. Geophys. Res. Planets* **2007**, *112*, E12. [CrossRef]
170. Gasnault, O.; Taylor, G.J.; Karunatillake, S.; Dohm, J.; Newsom, H.; Forni, O.; Pinet, P.; Boynton, W.V. Quantitative geochemical mapping of Martian elemental provinces. *Icarus* **2010**, *207*, 226–247. [CrossRef]
171. Meslin, P.-Y.; Gasnault, O.; Forni, O.; Schröder, S.; Cousin, A.; Berger, G.; Clegg, S.M.; Lasue, J.; Maurice, S.; Sautter, V.; et al. Soil Diversity and Hydration as Observed by ChemCam at Gale Crater, Mars. *Science* **2013**, *341*, 1238670. [CrossRef] [PubMed]
172. McSween, H.Y., Jr.; Taylor, G.J.; Wyatt, M.B. Elemental composition of the Martian Crust. *Science* **2009**, *324*, 736–739. [CrossRef] [PubMed]
173. Agee, C.B.; Wilson, N.V.; McCubbin, F.M.; Ziegler, K.; Polyak, V.J.; Sharp, Z.D.; Asmerom, Y.; Nunn, M.H.; Shaheen, R.; Thiemens, M.H.; et al. Unique Meteorite from Early Amazonian Mars: Water-Rich Basaltic Breccia Northwest Africa 7034. *Science* **2013**, *339*, 780–785. [CrossRef] [PubMed]
174. Humayun, M.; Nemchin, A.; Zanda, B.; Hewins, R.H.; Grange, M.; Kennedy, A.; Lorand, J.P.; Goepel, C.; Fieni, C.; Pont, S.; et al. Origin and age of the earliest Martian crust from meteorite NWA 7533. *Nature* **2013**, *503*, 513–517. [CrossRef] [PubMed]
175. Wittmann, A.; Korotev, R.L.; Jolliff, B.L.; Irving, A.J.; Moser, D.E.; Barker, I.; Rumble, D. Petrography and composition of Martian regolith breccia meteorite Northwest Africa 7475. *Meteorit. Planet. Sci.* **2015**, *50*, 326–352. [CrossRef]
176. Liu, Y.; Ma, C.; Beckett, J.R.; Chen, Y.; Guan, Y. Rare-earth element minerals in Martian breccia meteorites NWA 7034 and 7533: Implications for fluid-rock interaction in the Martian crust. *Earth Planet. Sci. Lett.* **2016**, *451*, 251–262. [CrossRef]
177. The Martian Meteorite Compendium. Available online: https://curator.jsc.nasa.gov/antmet/mmc/ (accessed on 21 August).
178. Shearer, C.K.; Burger, P.V.; Papike, J.J.; McCubbin, F.M.; Bell, A.S. Crystal chemistry of merrillite from Martian meteorites: Mineralogical recorders of magmatic processes and planetary differentiation. *Meteorit. Planet. Sci.* **2015**, *50*, 649–673. [CrossRef]
179. Symes, S.J.; Borg, L.E.; Shearer, C.K.; Irving, A.J. The age of the Martian meteorite Northwest Africa 1195 and the differentiation history of the shergottites. *Geochim. Cosmochim. Acta* **2008**, *72*, 1696–1710. [CrossRef]
180. Treiman, A.H. The parent magma of Nakhla (SNC) meteorite, inferred from magmatic inclusions. *Geochim. Cosmochim. Acta* **1993**, *57*, 4753–4767. [CrossRef]
181. Treiman, A.H. The nakhlite meteorites: Augite-rich igneous rocks from Mars. *Chem. Erde-Geochem.* **2005**, *65*, 203–270. [CrossRef]

182. Jones, J.H. Isotopic relationships among the shergottites, the nakhlites and Chassigny. In Proceedings of the 4th Lunar and Planetary Science Conference, Houston, TX, USA, 14–18 March 1988; pp. 465–474.
183. Nyquist, L.E.; Shih, C.-Y.; McCubbin, F.M.; Santos, A.R.; Shearer, C.K.; Peng, Z.X.; Burger, P.V.; Agee, C.B. Rb-Sr and Sm-Nd isotopic and REE studies of igneous components in the bulk matrix domain of Martian breccia Northwest Africa 7034. *Meteorit. Planet. Sci.* **2016**, *51*, 483–498. [CrossRef]
184. Shirai, N.; Ebihara, M. The Magmatism of Mars Inferred From Chemical Composition of Shergottites. In Proceedings of the 37th Lunar and Planetary Science Conference, Woodlands, TX, USA, 13–17 March 2006; p. 1917.
185. Liu, Y.; Ma, C. Monazite in Martian breccia meteorite NWA 7034. In Proceedings of the 8th International Mars Conference, Pasadena, CA, USA, 14–18 July 2014; p. 1250.
186. Liu, Y.; Ma, C. Monazite, chevkinite-perrierite and xenotime in Martian breccia meteorite NWA 7034. In Proceedings of the 46th Lunar Planetary Science Conference, Woodlands, TX, USA, 16–20 March 2015; p. 1287.
187. Dauphaus, N.; Pourmand, A. Thulium anomalies and rare earth element patterns in meteorites and Earth: Nebular fractionation and the nugget effect. *Geochim. Cosmochim. Acta* **2015**, *163*, 234–261. [CrossRef]
188. Floss, C.; Crozaz, G. Heterogeneous REE patterns in oldhamite from aubrites: Their nature and origin. *Geochim. Cosmochim. Acta* **1993**, *57*, 4039–4057. [CrossRef]
189. Terada, K.; Sano, Y. Ion microprobe U-Pb dating and REE analyses of phosphates in H4-chondrite, Yamato-74371. *Geophys. Res. Lett.* **2002**, *29*, 1460. [CrossRef]
190. Reed, S.J.B.; Smith, D.G.W.; Long, J.V.P. Rare earth elements in chondritic phosphates—Implications for ^{244}Pu chronology. *Nature* **1983**, *306*, 172–173. [CrossRef]
191. Martínez-Jiménez, M.; Moyano-Cambero, C.E.; Trigo-Rodríguezm, J.M.; Alonso-Azcárate, J.; Jordi, L. *Asteroid Mining: Mineral Resources in Undifferentiated Bodies from the Chemical Composition of Carbonaceous Chondrites*; Assessment and Mitigation of Asteroid Impact hazards, Astrophysics and Space Science Proceedings; Springer: New York, NY, USA, 2017; pp. 73–101.
192. USGS. Platinum-Group Elements-So Many Excellent Properties. 2014. Available online: https://pubs.usgs.gov/fs/2014/3064/pdf/fs2014-3064.pdf (accessed on 2 August 2017).
193. NASA Approves 2018 Launch of Mars InSight Mission. Available online: https://insight.jpl.nasa.gov/home.cfm (accessed on 21 August 2017).
194. Mars 2020 Mission Overview. Available online: https://mars.nasa.gov/mars2020/mission/overview (accessed on 21 August 2017).
195. Cofield, C. NASA's Mars Plan May Include Yearlong Mission to the Moon. 2017. Available online: https://www.space.com/36781-nasa-yearlong-crew-moon-mission-ahead-of-mars.html (accessed on 6 August 2017).
196. Progress in Defining the Deep Space Gateway and Transport Plan. Available online: https://www.nasa.gov/sites/default/files/atoms/files/nss_chart_v23.pdf (accessed on 21 August 2017).
197. Zubrin, R. The Case for Colonizing Mars. Ad Astra, 1996. Available online: http://www.ifa.hawaii.edu/~meech/a281/handouts/mars_case.pdf (accessed on 6 August 2017).
198. Wall, M. Private Mars Missions: A Red Planet Exploration Roundup. 2016. Available online: https://www.space.com/32721-private-mars-missions-spacex-red-dragon.html (accessed on 6 August 2017).
199. National Aeronautics and Space Administration. Available online: https://solarsystem.nasa.gov/missions/near/indepth (accessed on 21 August 2017).
200. Asteroid Explorer "HAYABUSA" (MUSES-C). Available online: http://global.jaxa.jp/projects/sat/muses_c/ (accessed on 21 August 2017).
201. Asteroid Explorer "Hayabusa2". Available online: http://global.jaxa.jp/projects/sat/hayabusa2/ (accessed on 21 August 2017).
202. OSIRIS-Rex. Available online: https://www.nasa.gov/osiris-rex (accessed on 21 August 2017).
203. Crawford, I.A. The long-term scientific benefits of a space economy. *Space Policy* **2016**, *37*, 58–61. [CrossRef]